C121W:
A THERMOSENSITIVE SODIUM CHANNEL MUTATION

by

Csilla Egri

B.Sc. (Kinesiology), Simon Fraser University, 2009

THESIS SUBMITTED IN PARTIAL FULFILLMENT OF
THE REQUIREMENTS FOR THE DEGREE OF

MASTER OF SCIENCE

in

School of Kinesiology

Department of Biomedical Physiology and Kinesiology

SIMON FRASER UNIVERSITY

Summer 2011

APPROVAL

Name: **Csilla Egri**

Degree: **M.Sc.**

Title of Thesis: **C121W: A Thermosensitive Sodium Channel Mutation**

Examining Committee:

Chair: **Dr. Glen Tibbits**
Professor and Chair, Biomedical Physiology and Kinesiology

_____

Dr. Peter Ruben
Senior Supervisor
Professor, Biomedical Physiology and Kinesiology

_____

Dr. Tom Claydon
Supervisory Committee Member
Assistant Professor, Biomedical Physiology and Kinesiology

_____

Dr. Charles Krieger
Supervisory Committee Member
Associate Professor, Biomedical Physiology and Kinesiology

_____

Dr. Harley Kurata
External Examiner
Assistant Professor, Anesthesiology Pharmacology and Therapeutics, UBC

_____

Date Defended/Approved: June 16, 2011

Declaration of
Partial Copyright Licence

ABSTRACT

A mutation in the β_1 subunit of the voltage-gated sodium (Na_V) channel, β_1(CW), causes genetic epilepsy with febrile seizures plus (GEFS+), wherein elevated body temperature increases neuronal excitability. This study investigated the putative mechanism underlying seizure generation in β_1(CW) caused by elevated temperature. Whole-cell voltage clamp experiments were performed on CHO cells expressing the α subunit of neuronal isoform $Na_V1.2$, either alone, with β_1, or with β_1(CW) at 22°C and 34°C . Results suggest that wild-type β_1 is protective against increased channel excitability induced by elevated temperature, and that this protection is lost in the absence of β_1 or with the expression of β_1(CW). At 34°C, β_1(CW) increased channel excitability compared to wild-type β_1 by decreasing use-dependent inactivation, increasing persistent current and window current, and delaying the onset of, and accelerating the recovery from, fast-inactivation. These results help explain how the β_1(CW) mutation contributes to the febrile seizure phenotype by increasing channel excitability specifically at elevated temperature.

Keywords: C121W; GEFS+; Sodium Channel; Temperature.

ACKNOWLEDGEMENTS

"I'd like to do my Directed Studies in your lab, Dr. Ruben, working with sodium channels seems very mysterious." Yes, those were my words; spoken as a 3rd year undergrad looking to fill my semester courseload. Although totally naïve to what scientific research actually entailed, I was right about the mystery. Not a kind of whodunit mystery, but that akin to a cleverly designed puzzle, and I full heartedly enjoyed the process of working towards its logical solution. Apparently I enjoyed it so much so, that one semester turned into two, two semesters turned into a summer research assistantship, and that summer turned into a two year commitment towards a Master's degree.

This thesis would not have been possible without that initial chance encounter with Peter in the Kinesiology main office 4 years ago, and the continued support, guidance, and inspiration offered throughout my undergraduate and graduate years. In addition to the major role that Peter has played, I would also like to thank everyone that has become part of what is my extended scientific family; Uncle Yuriy Vilin, Uncle Tom Claydon, Auntie Charlene Allard, Cousins Aaron Van Slyke and May Cheng, second Cousin Eric Lin, and step-brother David Jones. The process of working towards logical conclusions wouldn't have been nearly as productive or as much fun without the members of my ion channel family.

INTRODUCTION

Approximately 2-5% of children aged 6 months to 6 years experience convulsions in response to fever, and one third of those who experience a febrile seizure (FS) will have a recurrent attack[1,5]. Although generally considered benign, FSs are distressful to both family and child, and about 7% of children with FS will later develop recurrent unprovoked seizures (epilepsy)[2]. A possible explanation for the high incidence of FS in childhood is the heightened neuronal activity due to extensive synaptic pruning and network remodelling, potentially increasing the susceptibility of the immature brain to environmental perturbations[3]. A clinical subset of FS, genetic epilepsy with febrile seizures plus (GEFS+), is a pediatric epilepsy syndrome in which seizures are present with or without fever beyond the age of 6 (FS+). Genetic screening has revealed several mutations to neuronal proteins linked to FS and GEFS+, such as mutations to $GABA_A$ receptors of inhibitory interneurons and voltage gated sodium (Na_V) channels and their associated subunits[4].

Na_V channels are pore forming macromolecular complexes containing one α subunit, which conducts sodium specific current, and one or more regulatory β subunits. Channel structure and function is described in more detail in section 1.1. There are currently 10 known Na_V channel isoforms, with Na_V 1.1, 1.2, 1.3, and 1.6 collectively referred to as neuronal channels because of their high expression in the central nervous system. The sodium current conducted by Na_V channels is responsible for the initial rapid

depolarizing upstroke of an action potential; hence any mutational perturbations to their gating can greatly affect neuronal excitability[6]. One particular mutation associated with GEFS+; a cysteine to tryptophan substitution at position 121 (C121W) in the auxiliary β_1 subunit of Na_V channels, suggests that the mutational increase in neuronal excitability is also temperature sensitive[7].

Na_V channels display temperature sensitive behaviour, as their gating involves conformational changes to the protein, the rate of which is increases with added thermal energy[68]. The temperature sensitivity of the Na_V channel α subunit alone has been investigated previously[8-11], but not in conjunction with its auxiliary β_1 subunit, which modulates many aspects of channel function. This study focuses on temperature and β_1 subunit modulation of a particular channel property; slow inactivation (SI). This type of channel inactivation determines the proportion of channels available to activate with subsequent membrane depolarizations and has previously been shown to have a greater dependence on temperature than any other state transition[9, 12, 13]. The effect of temperature on the β_1(CW) mutation in neuronal Na_V channels has not yet been assessed, nor has the effect of this mutation on SI in a neuronal channel.

Results from this study will be important in bridging the gap between clinical manifestation and molecular mechanism of FSs and will add to the growing body of literature regarding channel behaviour at close to physiological temperatures. Understanding how temperature differentially affects gating of native channels as well as those implicated in temperature sensitive disorders can help design drugs specifically targeted to gating parameters which are most greatly affected. This specific targeting would reduce potential side effects of current antiepileptic drugs, and would be able to

"blanket treat" any other syndrome which has a similar perturbation to Na_V function. As quoted by Petrou and Berkovic, "…the time has come for resolving the biology of this common and frightening form of seizure"[4], and understanding temperature effects on brain channels is one important step.

TABLE OF CONTENTS

LIST OF TABLES AND FIGURES

GLOSSARY

Fast inactivation	Block of the ion permeating pore thru intracellular IFMT motif binding. Sodium current is inactivated within a matter of 1-2 milliseconds after activation.
Febrile seizure	"a seizure occurring in childhood after one month of age, associated with a febrile illness not caused by an infection of the central nervous system, without previous neonatal seizures or a previous unprovoked seizure, and not meeting criteria for other acute symptomatic seizures" (ILAE definition)
$GABA_A$ receptor	Ligand gated channels found in inhibitory interneurons that activate in response to the neurotransmitter gamma-aminobutyric acid, resulting in an influx of chloride and subsequent hyperpolarization of the membrane.
Persistent current	Small (0.5%-5% of peak transient current) non-inactivating inward current either due to a subpopulation of channels with slower inactivation kinetics, or impairment of FI.
Q_{10}	Temperature coefficient; the measure of the rate of change of a biological or chemical system as a consequence of increasing temperature by 10 °C. $$Q_{10} = \frac{R_2}{R_1}^{\left(\frac{10}{T2-T1}\right)}$$ Where R is the rate and T is the temperature in Celsius.
Slow inactivation	Inactivation of sodium current that is distinct from FI. Occurs in the range of seconds to minutes in response to sustained (greater than 500 ms) or repetitive depolarization.
Use-dependent inactivation	Accumulation of the sodium channel in the inactivated state in response to a train of depolarizing pulses.
$V_{1/2}$	Voltage at which there is half maximal channel activation or half maximal current amplitude.

LIST OF ABBREVIATIONS

AED – anti-epileptic drug

AP – action potential

AIS – axon initial segment

AU - arbitrary units

C121W, CW, β_1(CW) – cysteine tryptophan exchange at position 121 of β_1 subunit

CAM – cell adhesion molecule

CHO – Chinese hamster ovary

FI – fast inactivation

FS – febrile seizure

FS+ - febrile seizure plus

GABA – gamma-aminobutyric acid

GEFS+ - genetic epilepsy with febrile seizures plus

HEK – Human embryonic kidney

HRA – hyperthermia induced respiratory alkalosis

Ig - immunoglobulin

I_M – intermediate inactivation

I_{Na} – transient sodium current

I_{NaP} – persistent current

IFMT – isoleucine-phenylalanine-methionine-threonine

Na_V – voltage-gated sodium

Q_{10} – temperature coefficient

RMP – resting membrane potential

SEM – standard error of the mean

SI – slow inactivation

UDI – use-dependent inactivation

WT – wild-type

1: SODIUM CHANNELS: A BRIEF INTRODUCTION

1.1 Structure and Function

1.1.1 Alpha subunit

The large (260kDa) pore forming α subunit of Na_V channels consists of four homologous domains (D1-DIV) each with six trans-membrane spanning helices (S1-S6). Each α subunit typically associates with one to two β subunits, the function of which is discussed in the following section. The predicted secondary structure of a generic Na_V channel and associated β-subunit is illustrated in Figure 1.

Na_V channels span the cell membrane and are the main determinants of action potential (AP) initiation and propagation in electrically excitable cells. Segments S5-S6 and their extracellular linker (referred to as the p-region) constitute the Na^+ permeable pore and selectivity filter, allowing passage of Na^+ ions down their electrochemical gradient. Na_V channels are not constitutively open, but are gated by changes in membrane voltage. A high density of positively charged amino acids in the S4 segment of each domain allows the segment to shift in response to changes in the electric field, thus the S4 segments are referred to as the channels` "voltage sensors". This voltage-dependent conformational change initiates a series of events leading to channel activation. Shortly after channel activation, four hydrophobic amino acid residues (IFMT) located within the intracellular linker of DIII and DIV, also undergo a conformational change and bind to the S4-S5

cytoplasmic linker of DIII and DIV. This "fast-inactivation" (FI) blocks the ion permeating pore and inactivates transient sodium current (I_{Na}) within a matter of 1-2 milliseconds.

There is a small area of overlap between the voltage-dependence of inactivation and activation, where channels activate but have not yet completed FI. The small, non-inactivating current that flows during this voltage range is referred to as window current. Incomplete FI can also result in persistent current (I_{NaP}), which is observed as small (0.5-5% of transient current) residual current remaining after channel opening. The precise molecular manifestation of I_{NaP} remains unknown, but is thought to be due to a subpopulation of channels with slower or impaired inactivation kinetics. Na_V mutations which increase window current and, or I_{NaP} also increase cellular excitability[14].

Once in the FI state, channels can quickly recover within a range of 5-10 ms upon return to hyperpolarized potentials. The time course of entry into, and recovery from, FI determines channel availability for subsequent APs. Sodium channel FI is responsible for the absolute refractory period of an AP and allows AP to propagate in a unidirectional manner because previous channels have not yet recovered from FI and cannot be re-activated.

Another form of channel inactivation, termed slow inactivation (SI), develops more slowly, in the range of seconds to minutes, in response to sustained (greater than 500 ms) depolarizations. Similar to SI onset, recovery from SI is also slow, occurring in the range of seconds to minutes at hyperpolarized potentials. Channels can enter a subset of SI as well, called intermediate inactivation (I_M), from which recovery shows intermediate kinetics (100ms to 1s). Although the recovery kinetics of I_M are distinct from both FI and SI, the molecular mechanism of this type of inactivation is unknown. Movement of the outer pore

segment is thought to facilitate I_M[15, 16], while movement of the outer pore as well as further movements of the S4 segments are thought to underlie SI[17,18]. These structural changes alter the configuration of the permeation pathway resulting in inactivation of current.

Finally, another subset of SI, termed use-dependent inactivation (UDI), occurs in response to repetitive membrane depolarizations. The duration of the depolarizing stimuli determines the relative contribution of inactivated states to current decay. Shorter duration pulse trains (less than 500ms) reflect accumulation of channels into the FI state, while I_M and use-dependent SI contribute more-so during longer duration stimuli. This activity dependent current decay is an important regulator of cellular excitability in high frequency firing neurons as it dictates the number of channels available to open in response to subsequent depolarizations. Any changes to the maximum probability of UDI would have profound consequences on neuronal excitability.

1.1.2 β subunits

Each α subunit is capable of associated with up to two β subunits, one covalently (β_2 or β_4) and one non-covalently (β_1 or β3), however the exact location of these interactions is yet to be determined[100]. Beta subunits are significantly smaller (33-36kDa) than the pore forming α subunit and are composed of an N-terminal extracellular immunoglobulin (Ig)-like domain, one α-helical transmembrane segment, and a short intracellular C-terminal tail. Cysteine residues at positions 21 and 121 (as predicted by amino acid numbering for the β_1 subunit)[21] form a disulfide bridge important in maintaining the looped configuration of the Ig-like domain (illustrated as blue line in Figure 1). The presence of this domain classifies β subunits as part of the immunoglobulin superfamily of cell adhesion molecules (CAMs). Similar to the function of CAMs, β subunits interact with many extracellular matrix proteins

and facilitate cellular aggregation as well as targeting and anchoring of Na_V channels to specialized areas of the cell membrane[20]. In addition to these functions, β subunits are also important modulators of channel voltage-dependence and gating.

This study investigates the effects of β_1 and the β_1(CW) mutant, therefore focus will be directed on reviewing β_1`s modulatory role (see Patino and Isom 2010[100] for a review of β2-4) . The non-covalent interactions between β_1 and the α subunit are predicted to occur both intracellularly and extracellularly[21, 97]. Studies using *Xenopus* oocytes suggest extracellular interactions occur between the β_1 Ig-domain and the S5-S6 linker on DI and DIV of the α subunit[22,23]. Cleaving the intracellular segment of β_1, however, abolishes α-β interaction in mammalian cells[24], and mutations on the intracellular C-terminal tail of the α subunit also appear to reduce α-β interaction[25, 26]. Regions predicted to be important in α-β interactions are illustrated in Figure 1 as red circles.

Figure 1. Secondary structure of sodium channel α and β subunit.

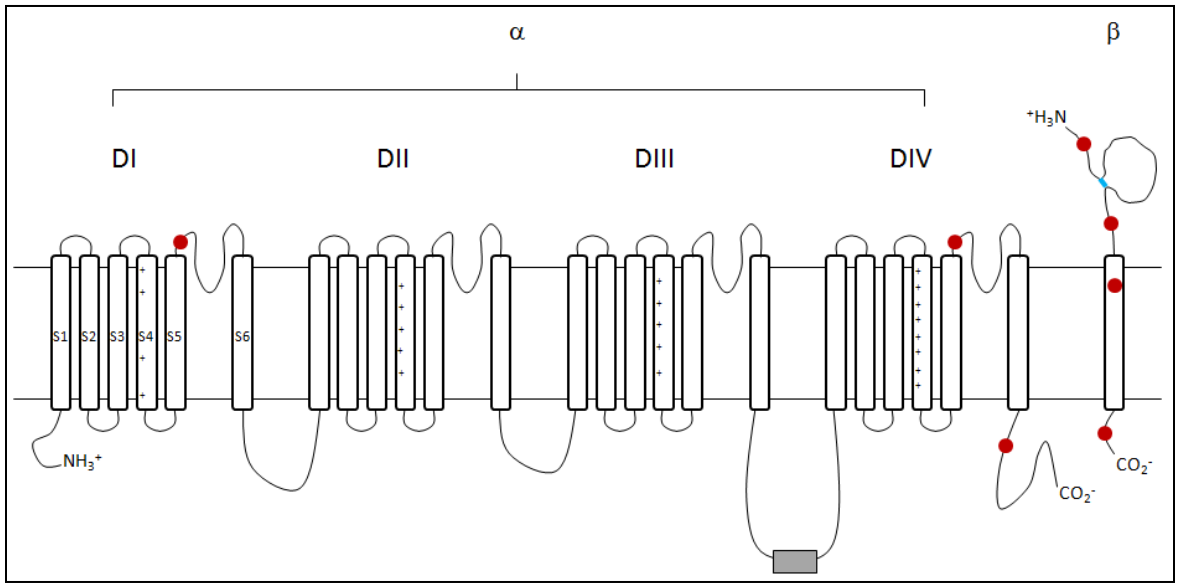

Schematic of predicted secondary structure for a generic Na_V channel pore forming α subunit and associated β subunit. Alpha helicies are depicted as cylinders, with connecting lines representing intracellular and extracellular linkers. Segments S1-S6 are labelled in domain I (DI) of the α subunit, and the high density of positively charged amino acid residues in the S4 segments are illustrated as plus signs spanning the α-helicies of each respective S4. The series of hydrophobic amino acid residues (IFMT) that constitute the fast inactivation particle is shown as a grey box on the intracellular linker between DIII and DIV. The Ig-like domain of the β subunit is shown as an extracellular loop, with the putative disulfide bridge between residues 21 and 121 shown as a blue line. Regions predicted to be important in α-β interactions are shown as red dots. Figure was generated using data from references 20-26.

The role of the β_1 subunit in channel gating and kinetics differs depending on the Na_V channel α subunit (neuronal, cardiac, skeletal) and the expression system used. Major differences occur between mammalian Chinese Hamster Ovary (CHO) cells or Human Embryonic Kidney (HEK) cells and amphibian *Xenopus laevis* oocytes. Sodium channels expressed in oocytes have abnormally slow gating kinetics without the co-expression of β_1, hence oocyte data suggests that the major role for β_1 is to modulate FI[21, 27]. The rate of FI in mammalian cells on the other hand, is not increased by β_1 because mammalian cells display fast Na_V channel gating even without β_1[28-31] (but see [32, 33]). For this reason, oocyte expression systems may not be the best suited for studying β_1 function, let alone

pathophysiological nature of β_1 mutations. Unfortunately, even among mammalian expression systems, the role of β_1 in Na_V channel function is varied. The high variability might be due to differing expression levels of endogenous β subunits in different cell backgrounds, variable compositions of the cell membrane (phospholipid content and microdomains), as well as cell-type specific glycosilation and phosphorylation pathways, all which have been shown to modulate β function[100].

The effects of β_1 on voltage-dependence of activation range from a depolarizing shift[21, 29, 33] to a hyperpolarizing shift[34, 35], to no effect at all[30, 32, 36, 37]. There are similar inconclusive results for voltage-dependence of FI; β_1 induced depolarizing shift[30], or hyperpolarizing shift[30, 34-36]. Further discrepancies exist in β_1's role in UDI of Na_V channels, with observations showing either an increase in UDI (a greater decrease in current after a train of depolarizing pulses)[30] or a decrease in UDI[33]. A consistent depolarizing shift, however, seems to be apparent in the voltage-dependence of SI in $Na_V1.4$ or $Na_V1.2$ co-expressed with β_1[33, 37]. The probability of steady-state SI also seems to increase with β_1 in $Na_V1.4$, but this is not universal across all channel isoforms, as β_1 does not appear to affect steady-state SI in $Na_V1.5$[17]. A role for β_1 that seems to have some consensus is that it increases cell surface expression of Na_V channels[29-31], however this is not fully understood in heterologous expression systems, as addition of the β_1 subunit does not always lead to increased peak current[30, 32]. The level of I_{NaP} also seems to decrease with co-expression of β_1, an effect that would reduce cellular excitability by decreasing the steady inward depolarizing current[32, 35, 38], but again, this finding is not universal[28, 30, 36].

Although heterologous expressions systems yield inconclusive results for the specific modulatory role of β_1, SCN1B null mice, which lack β_1 subunits, demonstrate that

β_1 is crucial for normal neuronal development, excitability, and architecture[39]. Furthermore, mutations to β_1 cause many human disorders such as GEFS+, temporal lobe epilepsy, and cardiac conduction diseases such as Brugada syndrome[40-42].

1.2 Localization of the alpha subunit

To date, 10 mammalian isoforms of Na_V channel α subunits have been found, each with slightly modified functionality. Typically, $Na_V1.1$, 1.2, 1.3, and 1.6 are preferentially expressed in the central nervous system, 1.7, 1.8, 1.9 and Na_VX in the peripheral nervous system, 1.4 in skeletal muscle, and 1.5 in cardiac muscle. The differential expression of Na_V channel isoforms often leads to their description as "neuronal", "cardiac", or "skeletal". Each isoform can, however, be expressed diffusely throughout the body, so this kind of terminology is becoming a less accurate depiction of Na_V channel localization.

1.2.1 Function related to cellular localization

The target organ of this study is the brain, thus attention will given to description and characterization of 'neuronal' Na_V channel isoforms and their involvement in seizure genesis.

As mentioned previously, Na_V channels are critical components of AP initiation and propagation. The site of AP generation is the axon, specifically the distal portion of the axon initial segment (AIS)[43, 44]. Antibody staining, voltage clamp, and imaging studies show that Na_V channel expression is almost 50 times higher in the AIS than in the dendrite or the soma[45]. The high density of Na_V channels allows for the threshold of AP generation to be at least 15mV lower than elsewhere on the neuron[43,46]. The specific channel isoforms that localized to the AIS are $Na_V1.2$ and $Na_V1.6$[8, 45].

The expression and biophysical properties of each isoform may change, however, due to developmentally regulated splicing of Na_V channel genes. $Na_V1.3$ and $Na_V1.2$ have both adult and neonate splice variants, and adult $Na_V1.2$ has been shown to have increased excitability compared to its neonate counterpart[47]. The relative excitability of each variant may have implications in seizure genesis, but the mechanisms have yet to be worked out.

Isoform expression levels also appear to be affected by seizure activity, as mRNA levels of neonatal $Na_V1.2$ and $Na_V1.3$ are reported to increase after induced seizures in adult rats[48]. Human epileptic hippocampal tissue also shows up-regulated $Na_V1.3$ mRNA, and epileptic rat brain slices reveal increased protein amounts of $Na_V1.1$ and β_1[49,50]. In contrast, down-regulation of $Na_V1.2$ mRNA is observed in human epileptic tissue, so whether or not channel proteins increase or decrease with seizure may depend on the seizure mechanism[51]. Although there are many reports of altered channel expression after seizures, it is not known whether it is a causative agent or a result of the epileptic condition and/or treatment with antiepileptic drugs. Nevertheless, implications of $Na_V1.2$ and β_1 in neuronal plasticity after seizures further adds to the physiological relevance of this study.

1.3 Temperature Sensitivity

Due to the technical challenges associated with performing electrophysiological experiments at physiological temperatures, most of what is known about Na_V channel function has been collected at room temperature (ca. 20-22˚C). However, channel gating is temperature sensitive; the rates of Na_V channel activation, deactivation, FI, and SI all increase at higher temperature[8, 9, 52], with the rate of inactivation affected to a greater degree than activation[53]. This change in rate with increased temperature is described by the

temperature coefficient, Q_{10}, which ranges between 2-4 for Na_V channels[6]. In contrast, conductance through an open channel is relatively temperature insensitive, with a Q_{10} value of about 1.4, similar to aqueous diffusion, and simply reflects changes to the viscosity of water altering ionic flux[6]. The heat-induced acceleration of gating kinetics is not a surprising phenomenon, as added thermal energy would decrease the activation energy needed for conformational changes of the protein to occur. The transition of Na_V channels from one state to another each have independent rate constants, thus the Q_{10} of these processes should be determined individually[54]. Hodgkin and Katz demonstrated this phenomenon in 1949, showing a greater slowing of channel inactivation than activation in response to cooling of the axonal membrane[53]. This effect may vary between channel isoforms, however, as AP modelling of $Na_V1.5$ show that temperature induced changes to current are only reproducible if the Q_{10} value for activation is larger than that for inactivation[55].

Whether or not temperature affects the voltage-dependence of gating in native channels is debatable. A large number of studies show little or no effect of temperature on the $V_{1/2}$ of steady-state activation[9, 10, 55-58], while others show a heat-induced hyperpolarizing shift in $V_{1/2}$ of activation[8, 59]. The $V_{1/2}$ of inactivation, and especially SI, seems to show stronger temperature sensitivity[9, 12, 13, 52, 60, 61]. The larger temperature sensitivity of SI may reflect the greater number of state transitions required to complete SI in comparison to FI[19, 62]. The direction of heat-induced shift varies, however, depending on the experimental conditions. Increased temperature has been stated to cause either depolarizing shift in $V_{1/2}$ of steady-state SI[9,12] or a hyperpolarizing shift[63]. A depolarizing shift in $V_{1/2}$ of SI would mean that at 22˚C, at the resting membrane potential (RMP; approximately -60 mV for

neuronal cells), most channels are in the SI state, whereas at physiological temperature, a greater proportion of channels would be available for activation at RMP[9].

Thomas *et. al*[8] studied temperature sensitivity of neuronal $Na_V1.2$ at 22˚C, 37˚C, and 41˚C and showed via computer modelling of a dentate gyrus granule cell that increased temperature causes a direct increase in cellular excitability. Among the heat-induced increases in gating rates (FI and activation), a hyperpolarizing shift in the $V_{1/2}$ of activation was observed between 37˚Cand 41˚C, indicating that at a constant voltage, heat alone could activate channels. AP modelling revealed that the increased rate of FI onset and recovery combined with hyperpolarizing shift in $V_{1/2}$ of activation lowered the threshold for AP firing and increased firing frequency.

Thomas *et. al*[8] conclude that $Na_V1.2$ is a highly thermosensitive channel, and that heat alone may open channels by hyperpolarizing the $V_{1/2}$ of activation. Although their results suggest that $Na_V1.2$ is implicated in FS etiology, they did not co-express $Na_V1.2$ with its regulatory β_1 subunit, and the present study shows that the β_1 subunit has a significant thermoprotective effect. They also did not assess recovery from inactivation, which the present study shows has a different temperature sensitivity to that of inactivation onset. The unique temperature dependencies of recovery and onset are required to predict the effect of elevated temperature on high frequency firing neurons in which Na_V channels accumulate into a combination of inactivated states (UDI)

Temperature studies on UDI, along with other components of SI, are scarce due to the technical challenges associated with maintaining adequate voltage control, and cell viability at elevated temperatures long enough to measure SI properties. The present study characterizes the effect of temperature on UDI along with relative rates of onset and

recovery from steady-state SI. This is important, because if inferences are to be made in regards to the role of Na_V channels in epileptogenesis, we must understand how such biophysical parameters are affected at close to physiological temperature.

2: FEBRILE SEIZURES: THE STORY SO FAR

2.1 Familial Febrile Seizures

Febrile seizures (FS) are quite common in the general population, occurring in approximately 2-5% of children aged 6 months to 5 years[1]. The infant brain is known to be more sensitive to perturbations in homeostasis due to extensive neuronal network development and remodelling, but why some children respond to fever by seizing and some don't is still unknown. Genetic predisposition is a likely factor, as the incidence of FS and recurring FS is higher in patients with a family history of epilepsy or prior FS[64]. Mutations have been mapped to several chromosomal loci[65-70], as well as specific mutations to genes SCN1A and SCN9A encoding Na_V channel isoforms 1.1 and 1.7[71-73].

Increased temperature sensitivity, either of the immature brain or due to mutations, is a likely mechanism of FS. Other factors may also be involved in seizure genesis. Inflammatory cytokines produced during infection and fever may increase neuronal excitability, or electrolyte imbalances during febrile states may perturb ionic homeostasis[74, 75]. Another possible precedent for seizure onset is increased intracortical pH due to hyperthermia-induced respiratory alkalosis (HRA)[76-78]. Although HRA involvement in seizure genesis is documented in animals, the extent of this effect is controversial in humans[79].

FS mechanism is probably a heterogeneous phenomenon, involving multiple mechanism and pathways. In spite of an unknown mechanism, elevations in body

temperature no doubt affect metabolism and cellular function, implicating the importance of hyperthermia in FS genesis. Hyperthermia-induced seizures in rat pups is a well-documented phenomenon, and this neuronal hyperexcitability is supported by AP recordings from rat brains[80-84]. Young rat hippocampal tissue slices heated by 3-4º produce ictal-like discharges, which disappear upon returning to baseline temperature[85]. Both such *in vivo* and *in vitro* analyses show age-dependent seizure activity, reflecting observations in humans[85].

Evidently, increased temperature can perturb the neuronal network enough to cause seizures. To date, no *in vitro* experiments have been performed investigating the effects of temperature on any specific Na_V channels mutation associated with familial FS. Clearly, temperature plays a major role in increasing neuronal excitability; therefore characterizing the temperature sensitivity of FS mutations would help clarify the mechanisms of this disease at the molecular level.

2.2 Genetic Epilepsy with Febrile Seizures Plus

Genetic epilepsy with febrile seizures plus (GEFS+) is a clinical subset of familial febrile seizures in which FS is the most common phenotype, followed by FS plus which persists beyond the age of six. In addition to FS, patients can display a large spectrum of unprovoked seizure disorders, such as atonic seizures, myoclonic-astatic epilepsy, and even as severe as myoclonic epilepsy of infancy or Dravet syndrome[86-88]. Because of the large clinical spectrum of GEFS+, the prevalence of this syndrome is difficult to determine, but specific genetic links to GEFS+ have been identified based on large families with multiple affected inidividuals[88]. GEFS+ is inherited in an autosomal dominant manner with incomplete penetrance, and the genetic heterogeneity of GEFS+ (meaning that different

mutations can give rise to same clinical phenotype) led to the classification of GEFS+ into seven different subtypes based on specific mutations. GEFS+ Type1 is associated with mutations to SCN1B encoding the β_1 subunit of Na_V channels, GEFS+ Type 2 with $Na_V1.1$, GEFS+ Type 3 with $GABA_A$ receptor γ_2, GEFS+ Type 5 with $GABA_A$ receptor δ, and GEFS+ Type 7 with $Na_V1.7$[89-91]. On top of the mutations to different genes, the GEFS+ phenotype is an outcome of different mutations to a single gene, for example, SCN1A encoding $Na_V1.1$ has over 20 identified mutations, each causing unique changes to Na_V channel function[92].

Each of the SCN1A mutations occurs at different locations throughout the channel and, not surprisingly, causes different functional changes. Studies using heterologous expression system reveal functional changes such as incomplete channel inactivation, increase I_{NaP}, or shifts in $V_{1/2}$ of activation and inactivation[92]. The variety of perturbations to channel function poses a problem in predicting disease mechanism, as opposing changes to the same phenomenon (increased or decreased entry into SI caused by two different mutations) still lead to the same clinical phenotype. In addition, the same mutation can yield two opposite phenotypes, either hypoexcitable or hyperexcitable neurons, depending on the cell type in which it is expressed[93].

Analysis of the functional effects of β_1 subunit mutations also yield inconclusive results. To date, five mutations to the β_1 subunit associated with the GEFS+ spectrum of disorders have been found, and four have been characterized *in vitro* (I70_E74del has yet to be characterized)[122]. Two mutations, a cysteine-to-tryptophan mutation at position 121 (C121W) and an arginine-to-histidine and/or cysteine exchange at position 85 (R85H/C) occur in the Ig-like loop of the extracellular domain[33, 41], and an arginine to cysteine

exchange at position 125 (R125C) occurs a few amino acids from C121W in the extracellular portion of β_1 (Fig 2.)[94].

Figure 2. SCN1B subunit mutations associated with GEFS+

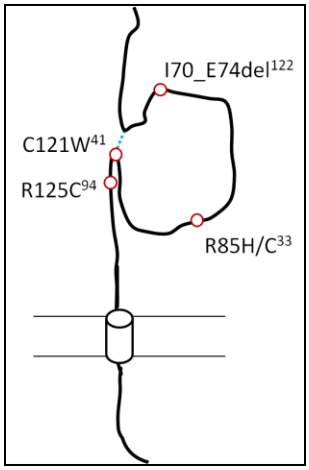

SCNIB mutations associated with the GEFS+ spectrum of disorders and their predicted locations on the β_1 subunit. All mutations occur on the extracellular portion of the β_1 subunit. Note the location of the C121W, predicted to disrupt the putative disulfide bridge holding the Ig-like domain together. The five amino acid deletion I70_E74del is associated with Dravet syndrome, but the functional consequence of this mutation has not yet been characterized in vitro. Superscripts indicate references for each respective mutation.

Interestingly, expression of the R85H/C or R125C mutants in HEK cells yields no detectable levels of β_1 protein on the cell membrane, but the R85H mutation maintained modulation of slow inactivation similar to wild-type β_1[33, 94]. These results suggest that subcellular interactions or very low surface protein expression (levels below immunohistochemical detection) may be sufficient to modulate some aspects of Na_V gating. Expression in an amphibian heterologous expression system can increase the amount of protein expression on the membrane. This is perhaps due to the lower incubation temperature (19°C as opposed to 37°C for mammalian cells) which can stabilize mutant proteins and prevent degradation by the endoplasmic reticulum. In fact, expression of R125C in *Xenopus* oocytes restores modulation of Na_V channel function in the same manner as β_1(WT)[94]. Oocyte expression of the C121W mutation, on the other hand, shows that although β_1(CW) associates with the α subunit, it fails to increase the speed of FI compared to wild type β_1[30, 41, 95]. This is most likely not the seizure causing mechanism of

this mutation, as oocytes display abnormally slow Na_V channel gating compared to mammalian cells. Since mammalian cells have a more similar intracellular milieu to that of neurons, they are a better representation of Na_V channel β_1 subunit function *in situ* than are ooctyes. Expression of β_1(CW) in a variety of mammalian cells shows retained α-β_1 dimerization, but its effect on Na_V channel function varies across laboratories[27, 30-32].

CHO cells expressing $Na_V1.3$ show that β_1(CW) does not alter the $V_{1/2}$ of channel activation or the time course of onset of steady-state FI but does increase channel availability by causing a depolarizing shift in $V_{1/2}$ of closed state FI compared to wild type β_1[30]. This suggests that the mutation could increase cell excitability by increasing the fraction of available channels at a given membrane potential. β_1(CW) also increases recovery from FI as seen by decreased frequency dependent inactivation of I_{Na} in response to a train of rapid depolarizing pulses[30]. This reduced current rundown during high frequency channel activity would potentially increase neuronal excitability. This altered Na_V channel gating has potential implications regarding the efficacy of antiepileptic drugs. Sensitivity to phenytoin, for example, is reduced with the co-expression of the β_1(CW) mutation[96].

The β_1 subunit has other functions besides modulation of channel gating, therefore the epileptogenic mechanism of the β_1(CW) mutation could also be due to impairments of β_1's cell adhesion and Na_V channel recruitment properties. Because the β_1(CW) mutation occurs at position 121, the exchange from a cysteine to tryptophan results in a loss of disulfide bridge formation between amino acid residues 121 and 21, important in maintenance of the configuration of the Ig-like domain (see Fig. 2). Indeed, disruption of the Ig-like domain due to the β_1(CW) mutation shows impeded cellular aggregation and

adhesion when expression in *Drosophila* S2 cells[30]. Although adhesion properties are impaired, recruitment of the α subunits to the membrane is attributed to the intracellular C terminal segment of β_1[97], therefore the location of the β_1(CW) mutation is not predicted to impair this function. Several studies in cultured cells show similar effectiveness of β_1(CW) compared to β_1 in promoting α subunit surface expression[30, 31]. The mechanisms of cell surface expression in cultured cells and native neurons likely differ, as *in vivo* studies of β_1(CW) paint a slightly different picture for this mutant, one in which it is neither co-localized with the α-subunit, nor expressed on the plasma membrane.

Imaging of cortical neurons transfected with the β_1(CW) mutation show that although localized to the axon initial segment (AIS), β_1(CW) is retained in the cytosol and does not co-localize with the α subunit or ankyrin$_G$. This is interesting as, although β_1(CW) is not present on the membrane, expression of $Na_V1.1$, 1.2 and 1.6 at the AIS is unimpaired[7]. This implies that β_1 is not required for Na_V α subunit recruitment to the membrane *in vivo*, and ankyrin binding motifs on the α subunit itself are sufficient for this task[98]. Although Na_V channel expression was not impaired, the loss of β_1 in the homozygous and heterozygous β_1(CW) mice (WW and CW respectively) resulted in increased neuronal excitability in the form of lowered AP threshold and increased burst duration[7]. This is contrary to analysis of peripheral nerve fibres from GEFS+ patients with an identified β_1(CW) mutation, which displayed slightly hypoexcitable behaviour[99]. The increased AP threshold and refractory period in these neurons was attributed to decreased expression and/or depolarized shift in activation of Na_V channels due to loss of β_1 function (different from the mechanism described for the β_1(CW) mice). GEFS+ patients do not have any peripheral nerve dysfunction, so this paradoxical change to AP properties may be due to the

differential expression of α subunit isoforms in peripheral and central neurons. Nonetheless, patients harbouring this mutation have altered AP properties in comparison to controls, demonstrating that β_1(CW) can have widespread effects on neuronal excitability.

The most important clinical implication of β_1(CW) is its ability to precipitate FSs, a phenomenon which is reproducible in the β_1(CW) mouse model. Elevating core body temperature by streams of hot air showed a reduced thermal seizure threshold for both WW and CW mice, similar to that observed in GEFS+ and FS patients[7]. Although elevated temperature increased neuronal excitability in both WT and CW mice, AP generation and AP amplitude were increased to a greater extent in the CW mice[7]. Even more interesting is that significant differences between AP recordings from neurons of CW and WT mice were only observed at 34ºC and not at 22ºC, suggesting the effect of this mutation is unmasked at elevated temperatures[7].

3: RATIONALE

The exact role that Na_V channels and associated β_1 subunit play in FSs is not known, but mutations to these highly conserved proteins predispose individuals to FSs. We can work backwards from this information and try to answer the question*: do such mutations cause neuronal hyperexcitability during febrile states because they have an altered sensitivity to temperature?* Although there are limitations to investigating functional effects of mutations in heterologous expression systems, study of genetically manipulated animals is still only a model of what is a complicated human disorder. Even in studies on human tissue, subtle differences in neuronal morphology between peripheral and central neurons, and even within central neurons, makes it difficult to predict exact disease causing mechanisms. All three methods have nonetheless proven invaluable to understanding human disorders and advancing pharmacotherapy methods. This study adds to the growing body of FS literature by investigating the molecular aspects of the β_1(CW) mutation at elevated temperature.

3.1 Specific Aims

Aim 1: The effect of temperature on activation and FI in neuronal $Na_V1.2$ has been studied previously, but the effect of temperature on SI in $Na_V1.2$ is unknown. This study measures the effect of elevated temperature (34ºC vs. 22ºC) on biophysical properties of neuronal $Na_V1.2$, including steady-state SI, use-dependent inactivation (UDI), and the rate of onset and recovery from SI.

Aim2: Temperature sensitivity of $Na_V1.2$ in conjunction with the β_1 subunit has not yet been characterized. The β_1 subunit affects many aspects of channel function, thus likely modulates temperature sensitivity as well. This study investigates how co-expression of the β_1 subunit modulates the effects of temperature on $Na_V1.2$.

Aim3: The GEFS+ mutation, β_1(CW), increases susceptibility to FSs. The mechanism behind this increased susceptibility remains unknown, but it has been proposed that the β_1(CW) mutations causes the FS phenotype by altering the temperature sensitivity of native channels in comparison to wild-type β_1. This study compares how the co-expression of β_1(CW) affects $Na_V1.2$ properties compared to β_1 at both 22ºC and 34ºC.

3.2 Study Limitations

The following methodological limitations should be considered when interpreting results from this study and extrapolating them to the function of neurons *in situ* at physiological temperatures:

1. Two temperatures where used to assess the temperature sensitivity of channel function, 22°C and 34°C. To extrapolate results to physiological (37°C) and febrile (41°C) temperatures, I have assumed the effect of temperature on voltage-dependent properties of Na_V channels varies linearly from 22°C to 41°C. However, data would need to be collected at a minimum of three different temperatures to confirm such a linear temperature dependence.

2. Only the gating properties of Na_V channels were assessed in conjunction with the β_1 subunit. The β_1 subunit modulates not only the voltage-dependence and kinetics of Na_V channels, but also affects channel expression and localization, as

well as cell adhesion properties. The functional consequences of the β_1(CW) mutation at elevated temperature may extend beyond modification of channel gating.

3. Sodium channels can simultaneously associate with a β_2 or β_4 subunit in addition to a β_1 subunit. There is no evidence to suggest however, that either the β_2 or β_4 subunit can assume the role of β_1[100], therefore the effect of co-expression of other β subunits in conjunction with β_1(CW) was not assessed in the present study.

4. Although a mammalian expression system is better suited for study of β_1 function than *Xenopus* oocytes, there is evidence to suggest that the role of the β_1 subunit differs *in vitro* and *in vivo*[100]. Despite these differences, a heterologous expression system is, as of this date, the only practical way to assess the functional effects of the β_1 subunit on voltage-dependent and kinetic properties of a single Na_V channel isoform in isolation.

4: METHODS

4.1.1 β_1 subunits

Wild type (WT) rat β_1 is in a neo/kanamycin resistant pBK/CMV vector, suitable for transfection of mammalian cells. Plasmid DNA was amplified on kanamycin coated agar plates using competent HB101 *E. Coli* cells from Invitrogen. Mutant rat β_1(CW) was a gift from Dr. Lori Isom from Vanderbilt University, and is in an ampicillin resistant pcDNA3.1 vector. Mutant DNA was amplified on ampicillin coated agar plates using the same method as for β_1. A double digest of purified plasmid DNA was performed using BamHI and XHo1 restriction enzymes to ensure presence of appropriate sized (600kDa) mutant insert.

4.1.2 Cell Culture

Chinese Hamster Ovary (CHO) cells are an ideal expression system for studying the effects of the β_1 subunit, because unlike HEK cells, they have no detectable levels of endogenous β subunits[101, 102]. CHO cells stably expressing rat $Na_V1.2$ adult splice variant were a gift from Dr. Todd Scheuer from University of Washington. The rat $Na_V1.2$ ortholog has only a 2% amino acid sequence difference and the same kinetics as human $Na_V1.2$[103]. A stably expressing cell line has exogenous Na_V channel DNA incorporated into its own genome, thus transcription of Na_V channel DNA occurs with every cell replication. This method allows experiments to be performed on a population of cells uniformly expressing the $Na_V1.2$ protein, and is preferred over transient transfection of neuronal Na_V channels as they have tendency to spontaneously rearrange. CHO cells were maintained in Dulbecco's

modified Eagle's medium (DMEM-Invitrogen, Burlington, Ontario) supplemented with 5% fetal bovine serum (FBS-HyClone, Invitrogen) in the presence of 150µg/mL active G418 (BioShop, Burlington, Ontario) and 1000 units of penicillin/streptomycin (BioShop) in a humidified 5% CO_2 environment at 37˚C (HEPA Class II CO_2 Incubator – Thermo Scientific Nepean, Ontario) on 100mm tissue culture dishes. Culture media was changed twice a week, and cells were split twice a week to avoid 100% confluency.

4.1.2.1 Transfection

The β_1 subunit was transiently transfected into CHO cells prior to each recording. Stock culture cells from 100mm dishes were plated onto 60mm culture dishes once they reached 60-70% confluency. After the 60mm dishes reached 40-50% confluency, CHO cells were transfected with β_1 or β_1(CW) and eGFP DNA according to PolyFect transfection protocol (Invitrogen). Transfected cells were plated onto coverslips in a 35mm Petri dish. Recordings were performed morning after plating on coverslips to ensure adequate time for production and trafficking of proteins. Green fluorescent protein was used as a marker for successfully transfected cells, and only fluorescing cells were patched.

4.2 Electrophysiology

All whole cell current recordings were made using an EPC-9 amplifier, an ITC-16 interface (HEKA, Lambrecht, Germany) and an iMac running Patchmaster. Data were low pass filtered at 10kHz and sampled at 50KHz. A 50KHz sampling frequency samples current every 20µs, an adequate sampling rate even for accelerated channel kinetics at 34°C[8, 12, 104]. Pipettes were pulled from borosilicate glass capillaries (Sutter Instruments, Chicago, Illionois) using a Model P-1000 Puller (Sutter Instruments), coated in a thin layer

of dental wax and fire polished on a MF-830 microforge (Narishige, Japan) to a final tip resistance of 500kΩ-1.1MΩ. Pipette (intracellular) solution was composed of the following (in mM): 120 CsF, 20 CsCl, 10NaCl, and 10 HEPES adjusted to pH 7.4 with CsOH. Extracellular bath solution was composed of the following (in mM): 140 NaCl, 4 KCl, 2 $CaCl_2$, 1 $MgCl_2$, 10 HEPES adjusted to pH 7.4 with CsOH. CsF was used instead of CsCl in the internal solution to extend the life of the patch and maintain quality of the seal at 34ºC. The high electronegativity of the fluoride ion induces a hyperpolarizing shift in voltage-dependent properties compared to intracellular solutions using chloride, however channel kinetics remain the same[105]. Because the fluoride in the internal solution also acts as a phosphatase inhibitor as well as a calcium chelator, any regulatory effects on channel activity are removed[105].

Temperature of the bath solution (22ºC and 34ºC +/-0.15ºC) was controlled using a TC-10 temperature controller and an in-solution TH-80 thermistor (Dagan Corporation). The temperature effect on the HEPES buffered solution is -0.014 (dpH/d°C)[106], thus a 12°C change in temperature induces a -0.16 shift in pH. A -0.16 change in pH from pH 7.40 causes negligible effects to voltage-dependent properties of $Na_V1.2$[107] therefore data was not corrected for temperature induced shifts in pH.

Transfected cells remained in bath solution at set temperature for at least 10 min prior to gigaseal formation. Current recordings were only performed 5-6min after obtaining whole cell access due to time dependent increase in current seen with r$Na_V1.2$ expression in CHO cells[108]. Raising the temperature of the bath solution after whole cell access resulted in disruption of the patch due to thermal expansion of the apparatus in the recording chamber, therefore recordings could not be paired at two temperatures. Instead, a group of cells was

patched at 22ºC and then a new group at 34ºC. Series resistance compensation was not used during recording, as adequate voltage control was achieved by using low-resistance (500kΩ-1.1MΩ) coated pipettes. Only recordings which had a series resistance of less than 3.5MΩ were included in data analysis. For recordings from very small cells in which a series resistance of less than 3.5MΩ could not be achieved, electrical compensation of series resistance was used by adjusting values of the slow component of membrane capacitance. While electrical compensation decreases errors in voltage control, it can increase the time constant of membrane charging, potentially introducing time sensitive errors. No significant differences were found, however, between experiments with and without electrically compensated series resistance (Table A. Supplementary Figures and Tables).

4.2.1 Voltage Protocols

4.2.1.1 Voltage Dependence of Activation

Cells were held at -130mV and depolarized from -70mv to +70mV in 10mV steps for a duration of 20ms. Leak currents were compensated during recording with a P/4 leak subtraction protocol. This protocol measures the ohmic leak and capacity current, which is then subtracted from the voltage-dependent I_{Na}. A series of 4 hyperpolarizing voltage steps ¼ of the magnitude of those used to generate I_{Na} are performed after each pulse. Channel conductance (G) was then calculated from peak I_{Na} using

(Eqn 1). $$\textbf{Eqn1: } G_{Na} = \frac{I_{Na}}{V - E_{Na}}$$

where G_{Na} is conductance, I_{Na} is peak sodium current in response to V, the test pulse membrane potential, and E_{Na} is the equilibrium potential calculated from the Nernst equation.

Curves of conductance as a function of voltage were fit with a Boltzmann function (**Eqn2**).

$$\textbf{Eqn2: } {}^{G}/_{G_{max}} = 1 \Big/ \left(1 + exp\left(\frac{-ze_0\left(V_M - V_{\frac{1}{2}}\right)}{kT}\right)\right)$$

where G/G_{max} is normalized conductance amplitude, V_M is the test pulse membrane potential, z is the apparent valence, e_0 is the elementary charge, $V_{1/2}$ is the midpoint voltage, k is the Boltzmann constant and T is the temperature in K.

4.2.1.2 Persistent Current

Persistent current (I_{NaP}) was measured at the 45-50ms time interval during a 50ms depolarizing pulse to 0mV from a holding potential of -130mV. An average of 30 pulses was used to increase the signal to noise ratio.

4.2.1.3 Steady-State Fast Inactivation

Cells were stepped from -130mV to +20mV in 10mV increments for 500ms to FI channels, followed by a test pulse at -10mV for 19ms. Cells were recovered from FI between sweeps by a recovery pulse at -130mV for 20ms. Leak subtraction was performed online using a P/4 protocol. Normalized current amplitude as a function of voltage was fit with a modified Boltzmann equation (Eqn 5).

4.2.1.4 Open-State Fast Inactivation

The time constant (τ) for development of FI in the open state was derived using a single exponential fit from peak current to the end of the depolarizing pulse. Traces for which FI τs were reported include only those where a clear peak current was visible; from -20mV to +40mV.

4.2.1.5 Recovery from Fast Inactivation at -60mV

Cells were held at -130mV for 500ms prior to a step to 0mV for 500ms to FI channels. Recovery of current was measured at a 19ms pulse at -10mV following 12 intervals at -60mV ranging from 0-1.02s. Leak subtraction was performed online using a P/4 protocol. Time constants of FI recovery as a function of time showed two components and was best fit with a double exponential equation **(Eqn 4)**.

$$\textbf{Eqn4: } I = I_{ss} + \alpha_1 e^{\frac{-t}{\tau_1}} + \alpha_2 e^{\frac{-t}{\tau_2}}$$

where I is current amplitude, I_{ss} is steady state current or plateau amplitude, α_1 and α_2 are the amplitudes at time 0 for time constants τ_1 and τ_2, and t is time.

4.2.1.6 Use-Dependent Inactivation

Channels were accumulated into a use-dependent inactivated state by a 50Hz pulse train. The membrane was depolarized to 0mV for 5 ms with a 15ms interpulse duration at -60mV for a total of 1000 pulses (20s). This holding potential is roughly the resting membrane potential of neurons and the frequency of depolarizations represents moderate

neuronal AP firing. Leak subtraction was performed offline using Fitmaster. Normalized current amplitude as a function of time was fit with a double exponential equation up to 15s **(Eqn4).** Decreasing the double-exponential fit of UDI from 20s to 15s decreased the variability of fit by giving less weight to the oscillating inactivation during the latter portion of the inactivation protocol.

4.2.1.7 Voltage Dependence of Steady-State Slow Inactivation

Cells were held at -130mV and stepped from -110mV to +10mV in 10mV intervals for 50s. Cells were then quickly stepped to a 20ms hyperpolarizing pulse to -130mV to recover from FI, and stepped to a test potential of 0mV for 20ms. Leak subtraction was performed off-line using Igor Pro and Fitmaster. Channel availability as a function of prepulse voltage was fit with a modified Boltzmann equation (**Eqn5**) to account for the non-zero asymptote of SI.

$$\text{Eqn 5: } {}^{I}/_{I_{max}} = \frac{(I_1 - I_2)}{\left(1 + exp\left(\frac{-ze_0\left(V_M - V_{\frac{1}{2}}\right)}{kT}\right)\right)} + I_2$$

where I_{max} is maximum peak current, V_m is prepulse potential, $V_{1/2}$ is midpoint voltage, I_1 and I_2 are maximum and minimum values in the fit, e_o is elementary charge, z is apparent valence, k is the Boltzmann constant, and T is temperature in K.

4.2.1.8 Onset of Steady-State Slow Inactivation

From a holding potential of -130mV, cells were stepped to the conditioning voltage (+10mV) for increasing time intervals from 0-64s. The membrane was then hyperpolarized

back to -130mV for 20ms to recover from FI and stepped to a test potential of 0mV for 20ms. Leak subtraction was performed online using a P/4 protocol. Time constants of SI onset as a function of time were fit with a double exponential equation **(Eqn 4).**

4.2.1.9 Recovery from Steady-State Slow Inactivation

From a holding potential of -130mV, a 50s depolarizing pulse to 0mV was applied to fully SI channels. The cell was then hyperpolarized to -90mV for an alternating duration of time from 0-64s, stepped to -130 mV for 20ms to recover from FI, and peak current was tested at 20ms 0mV pulse. Leak subtraction was performed offline using Fitmaster. Time constants of SI recovery as a function of time were fit with a double exponential equation **(Eqn 4).**

4.2.2 Temperature coefficient Q_{10}

The temperature coefficient (Q_{10}) of channel properties was calculated using **Eqn 6**.

(Eqn 6)

$$Q_{10} = \frac{R_2}{R_1}^{\left(\frac{10}{T2-T1}\right)}$$

where R is the rate, estimated by $R=1/\tau$ where τ is the exponential time constant, and T is the temperature in Celsius. For voltage-dependent properties, R was substituted for the $V_{1/2}$ value.

4.2.3 Statistical Analysis

Bar charts were generated using SPSS for Windows (IBM Statistics Version 19) and statistical analysis was performed using JMP for Windows (SAS Institute Version 8.0.2). Statistical significance of mean values was determined using a two-way ANOVA with temperature and subunits as factors and temperature*subunits as the interaction term. When significance at $p < 0.05$ was detected, a Tukey's post hoc test was used to determine which of the six levels (three subunit variants at two temperatures) differed from each other. The biological variability of channel activity during long duration protocols produced large within group SEM's for some values derived from fit lines, therefore statistical significance could not be shown for all parameters at the $p < 0.05$ level. Some of the most variable fits to data included recovery from SSFI and SSSI, SI-onset, and UDI. A retrospective power-analysis of the slow component of UDI for example, reveals power as low as 14%, while less variable data, such as percentage of I_{NaP}, had a power of 70%. Low powered experiments have a low probability of rejecting the null hypothesis (H_0 = no difference between subunits or between temperature) and a higher probability of making a Type II error (accepting H_0 when in fact it is true). A larger sample size can decrease the SEM and increase the power of a test, therefore increasing the sensitivity of statistical analysis for highly variable parameters. The retrospective power analysis for time constants of UDI at $\alpha = 0.05$ estimates that an n of at least 30 is required for each subunit at each temperature to detect statistical significance. Such large sample sizes are outside the scope of this work.

5: RESULTS

5.1 Elevated temperature causes a hyperpolarizing shift in voltage-dependence of activation.

To test the hypothesis that the β_1(CW) mutation promotes febrile excitability by hyperpolarizing the voltage-dependence of activation at elevated temperatures, I measured the voltage-dependence of channel activation at 22°C and 34°C for $Na_V1.2+\beta_1$(WT), $Na_V1.2+\beta_1$(CW), as well as $Na_V1.2$ with no associated β_1 subunit. Figure 3A illustrates representative current traces in response to a series of depolarizing steps, and shows that macroscopic current decay is accelerated at elevated temperature. The corresponding current-voltage relationship is illustrated in Figure 3B, and shows that the membrane voltage which elicited peak I_{Na} was, on average, left shifted by 10mV in response to elevation in temperature (only data for $Na_V1.2$ shown). The reversal potential, as calculated from extrapolating the linear portion of the current voltage relationship, did not significantly differ among subunits or between temperatures, and ranged around 75±1mV. The reversal potential was used to calculated channel conductance as a function of membrane voltage (Eqn1). Normalized channel conductance was fit with a Boltzmann function for all subunits at 22°C (blue) and 34°C (pink) (Fig 3C). The wild-type or mutant β_1 subunits did not affect the $V_{1/2}$ of activation or slope factor (*k*) compared to $Na_V1.2$ alone. Elevated temperature, however, induced a significant hyperpolarizing shift in the average $V_{1/2}$ of activation for all subunits (Fig 3D, $p<0.01$), with $Na_V1.2+\beta_1$(CW) showing the greatest temperature induced shift (Fig 3B, $p<0.05$). The average Q_{10} value for the change in $V_{1/2}$ of activation was 1.2.

Elevated temperature also significantly increased the average slope factor for all subunits (Fig 3E, $p<0.05$).

Figure 3. Voltage-dependence of activation.

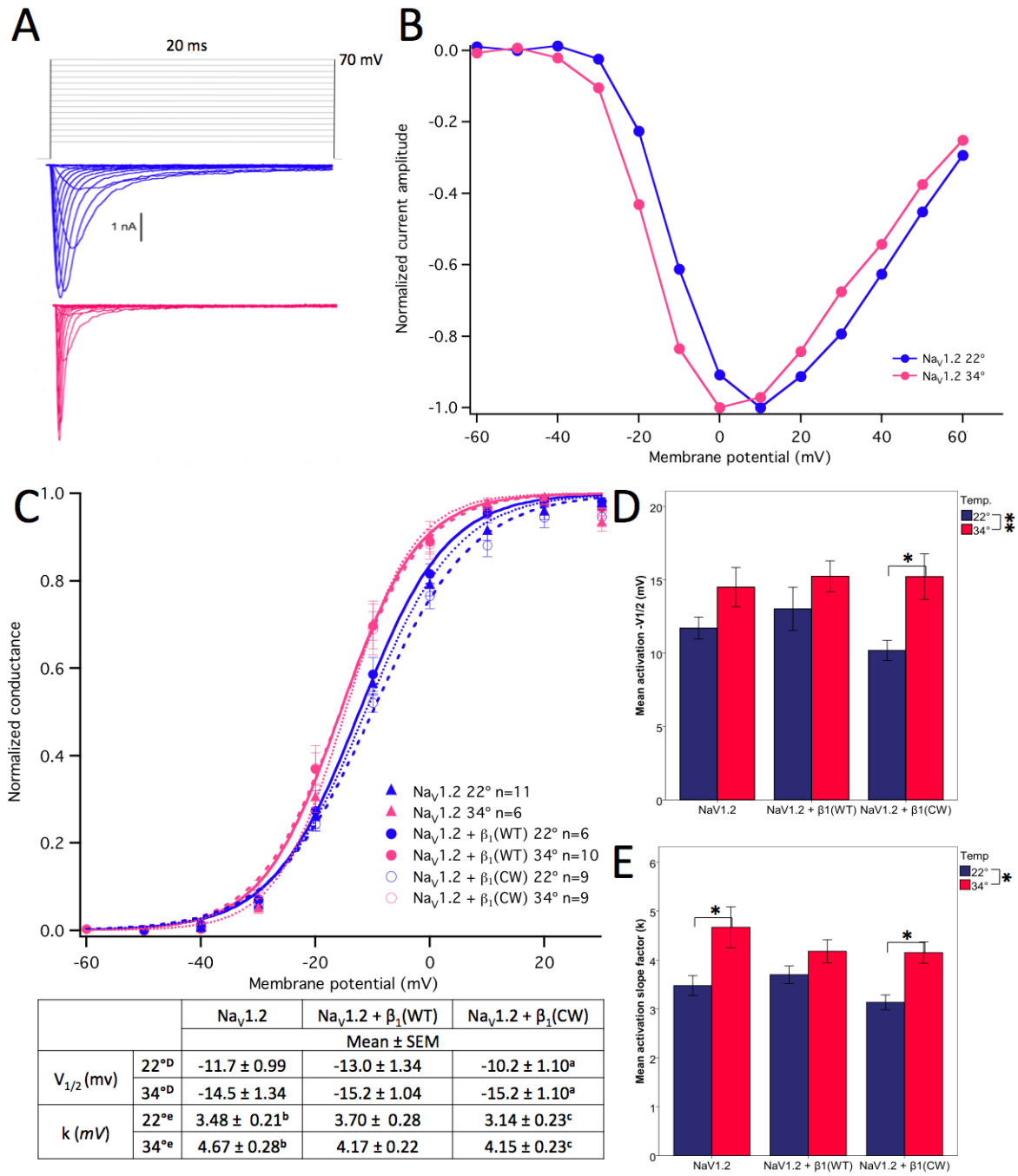

		Na$_V$1.2	Na$_V$1.2 + β$_1$(WT)	Na$_V$1.2 + β$_1$(CW)
		Mean ± SEM		
$V_{1/2}$ (mv)	22°^{D}	-11.7 ± 0.99	-13.0 ± 1.34	-10.2 ± 1.10^a
	34°^{D}	-14.5 ± 1.34	-15.2 ± 1.04	-15.2 ± 1.10^a
k (*mV*)	22°^{e}	3.48 ± 0.21^b	3.70 ± 0.28	3.14 ± 0.23^c
	34°^{e}	4.67 ± 0.28^b	4.17 ± 0.22	4.15 ± 0.23^c

A) Representative current traces from Na$_V$1.2 at 22°C (blue) and 34°C (pink) in response to voltage protocol shown (described in Methods). Elevated temperature accelerated

macroscopic current decay for all subunits (traces not shown) **B)** Normalized current-voltage (IV) relationship from current traces in A). No differences between IV relationships were observed between subunits (data not shown). The membrane voltage that elicited peak I_{Na} was left shifted at 34°C compared to 22°C (0mV and 10mV respectively, similar results for all subunits) **C)** Normalized conductance as a function of membrane voltage. Voltage protocol as described in Methods. Mean values of Boltzmann fits are displayed in the table. Matching superscript letters in the table indicate statistically significant difference at $p<0.05$, and capital superscripts indicate $p<0.01$. **D)** Mean $V_{1/2}$ values with ±1S.E.M. The averaged $V_{1/2}$ of activation for all subunits was significantly hyperpolarized by elevated temperature (-11.6mV ± 0.67mV, -15.0mV ± 0.67mV at 22°C and 34°C respectively; $p<0.01$) with the greatest temperature induced change occurring in $Na_V1.2 + \beta_1$(CW). **E)** Mean slope factors with ±1S.E.M. The averaged slope factor for all subunits was significantly increased at 34°C ($p<0.05$).

5.2 Mutant β_1(CW) destabilizes the FI state compared to wild-type β_1.

The temperature sensitivity of the voltage-dependence of steady-state FI was measured for all subunits to assess whether the β_1(CW) mutation increased febrile excitability by a reducing the proportion of channels in the FI state at a given membrane potential. Figure 4A illustrates steady-state FI for all subunits with Boltzmann fits at 22°C (blue) and 34°C (pink). The wild-type β_1 subunit causes a significant hyperpolarizing shift in the average $V_{1/2}$ of inactivation compared to $Na_V1.2$ alone (Fig 4B, $p<0.01$). The mutant β_1(CW) destabilized the FI state compared to β_1(WT), showing a more depolarized $V_{1/2}$ of inactivation compared to $Na_V1.2+\beta_1$(WT) ($p<0.05$), but still more hyperpolarized than $Na_V1.2$ ($p<0.01$). The $V_{1/2}$ of inactivation was also modulated by temperature, with a significant depolarizing shift at 34°C ($p<0.05$). The inactivation slope factor (*k*), on the other hand, appeared to be relatively insensitive to temperature except in $Na_V1.2+\beta_1$(WT) (Fig 4C). $Na_V1.2+\beta_1$(WT) had a significantly smaller slope factor than $Na_V1.2$ at 22°C ($p<0.05$), and showed approximately a 1mV increase at 34°C ($p<0.05$), becoming similar to that of $Na_V1.2$. The slope factor of $Na_V1.2+\beta_1$(CW) was significantly smaller than $Na_V1.2$ at both temperatures ($p<0.05$).

Figure 4. Steady-state FI.

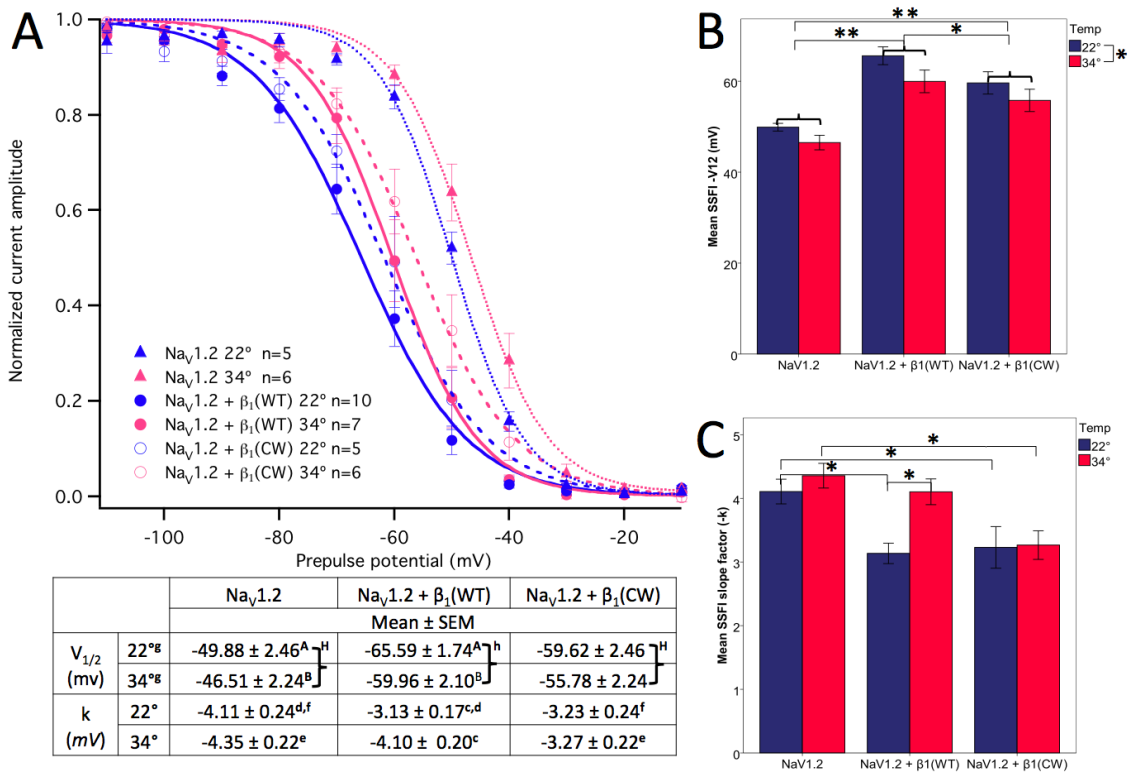

		$Na_V1.2$	$Na_V1.2 + \beta_1(WT)$	$Na_V1.2 + \beta_1(CW)$
		Mean ± SEM		
$V_{1/2}$ (mv)	22°[g]	-49.88 ± 2.46[A] [H]	-65.59 ± 1.74[A] [h]	-59.62 ± 2.46 [H]
	34°[g]	-46.51 ± 2.24[B]	-59.96 ± 2.10[B]	-55.78 ± 2.24
k (*mV*)	22°	-4.11 ± 0.24[d,f]	-3.13 ± 0.17[c,d]	-3.23 ± 0.24[f]
	34°	-4.35 ± 0.22[e]	-4.10 ± 0.20[c]	-3.27 ± 0.22[e]

A) Normalized current amplitude as a function of prepulse potential. Voltage protocol as described in Methods. Mean values of Boltzmann fits are displayed in the table. Matching superscript letters in the table indicate statistically significant difference at $p<0.05$, and capital superscripts indicate $p<0.01$.
B) Mean $V_{1/2}$ values with ±1S.E.M. Elevated temperature significantly depolarized the averaged midpoints for SSFI for all subunits (-54.0mV ± 1.3mV, -58.4mV ± 1.3mV, at 34°C and 22°C respectively; $p<0.05$). The averaged midpoint including both temperatures for $Na_V1.2$ was significantly more depolarized than $Na_V1.2 + \beta_1(CW)$ (-48.2mV ± 1.7mV, -57.7 ± 1.7mV respectively; $p<0.001$) and $Na_V1.2 + \beta_1(CW)$ was significantly more depolarized than $Na_V1.2 + \beta_1(WT)$ (-57.7 ± 1.7mV, -62.8 ± 1.4mV respectively; $p<0.05$).
C) Mean slope factors (*k*) with ±1S.E.M**.** $Na_V1.2$ had significantly greater *k* at 22°C than both $Na_V1.2 + \beta_1(WT)$ and $Na_V1.2 + \beta_1(CW)$ ($p<0.05$) and a greater *k* at 34°C than $Na_V1.2 + B_1(CW)$ ($p<0.05$). $Na_V1.2 + \beta_1(WT)$ was the only subunit with a significant increase in *k* with elevated temperature ($p<0.05$).

5.3 $Na_V1.2 + \beta_1$(CW) increases window current and persistent current at higher temperature.

To better understand how temperature induced shifts in channel activation as well as FI collectively influence channel excitability, I measured the area of window current for each subunit at both temperatures. Figure 5 illustrates window current as the overlay of the conductance and steady-state FI curves, with the inset showing the integrated area of overlap at 22°C (blue) and 34°C (pink) for $Na_V1.2+\beta_1$(WT) (left), $Na_V1.2+\beta_1$(CW) (middle) and $Na_V1.2$ (right). The peak normalized current amplitude at the intersection of the activation and inactivation curves was highest for $Na_V1.2$ and increased with temperature for both $Na_V1.2$ and $Na_V1.2 + \beta_1$(CW). Elevated temperature also increased the area of window current in $Na_V1.2+\beta_1$(CW) and $Na_V1.2$, but not in $Na_V1.2+\beta_1$(WT) (Fig 5 inset). Because the co-expression of either β_1(WT) or β_1(CW) results in a left shift of the $V_{1/2}$ of FI compared to $Na_V1.2$ alone, the voltage range at which window current occurred was more hyperpolarized compared to $Na_V1.2$ alone. The voltage range of window current did not overlap with voltage range of peak current (0mV to +10mV) for any subunit. To test whether temperature had an effect on persistent current (I_{NaP}) at peak, I measured residual current at 45ms of a 50ms depolarizing pulse to 0mV (Fig 6A). Elevating the temperature significantly increased the amplitude of I_{NaP} in $Na_V1.2+\beta_1$(CW) (Fig 6A and B, $p<0.05$). The amplitude of I_{NaP} appeared to decrease with temperature in $Na_V1.2$ however, (though this was not significantly different from 22°C), resulting in a lower level I_{NaP} than $Na_V1.2+\beta_1$(CW) at 34°C ($p<0.05$). A two-way ANOVA produced a significant interaction term between temperature and subunit ($p<0.05$) suggesting that the change in I_{NaP} varies with subunit and temperature.

Figure 5. Window current.

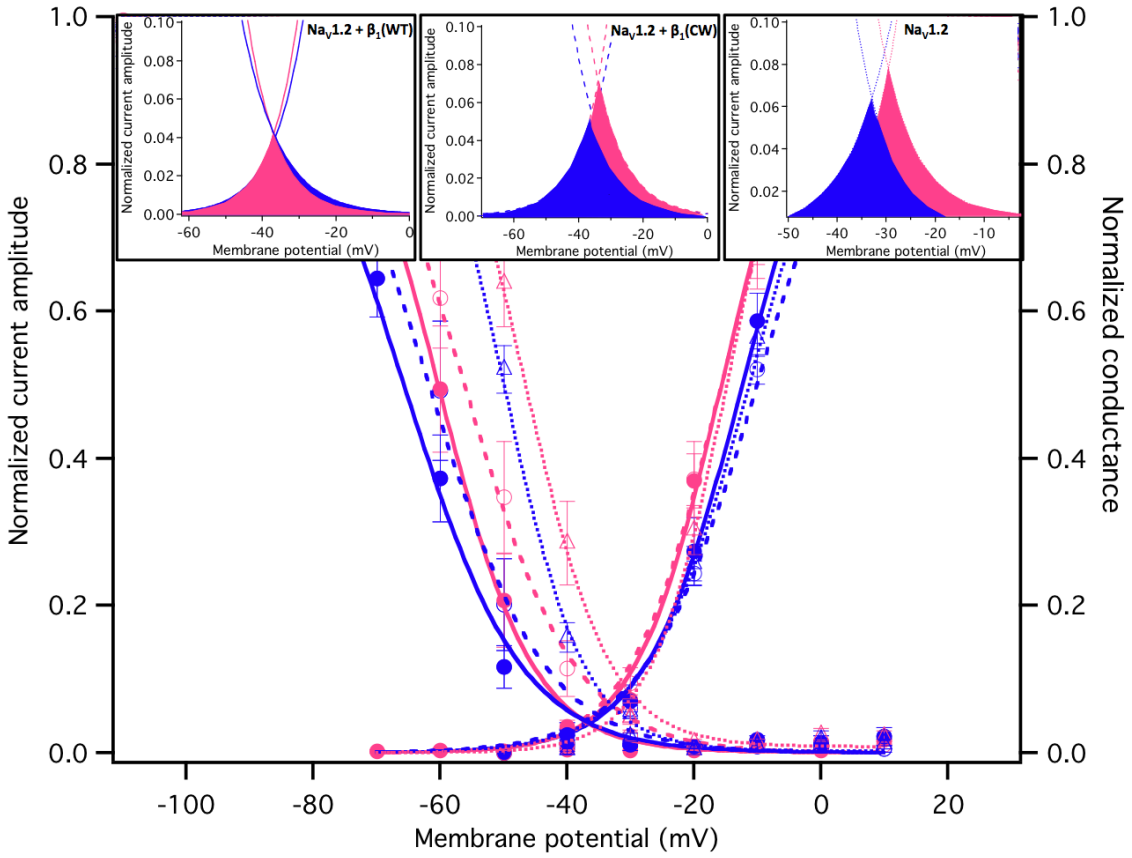

Window current was calculated at 22°C and 34°C by integrating the area under the overlay of the average Boltzmann fits for conductance and SSFI. **Inset:** Expanded view of window currents in at 22°C (blue) and 34°C (pink). Temperature increased the area of window current in both $Na_V1.2$ and $Na_V1.2 + \beta_1$(CW), but not in $Na_V1.2 + \beta_1$(WT). The area of window current measured in arbitrary units (AU) at 22°C and 34°C, respectively, is as follows; $Na_V1.2 + \beta_1$(WT) 0.69 AU, 0.67 AU; $Na_V1.2 + \beta_1$(CW) 0.85 AU, 1.16 AU; $Na_V1.2$ 0.85 AU,1.3 AU. The peak normalized current amplitude at the intersection of the activation and inactivation curves was highest for $Na_V1.2$ and increased with temperature for $Na_V1.2$ and $Na_V1.2 + \beta_1$(CW) (0.05, 0.07 for $Na_V1.2 + \beta_1$(CW) and 0.06 and 0.08 for $Na_V1.2$ at 22°C and 34°C respectively).

Figure 6. Persistent current (I_{NaP}).

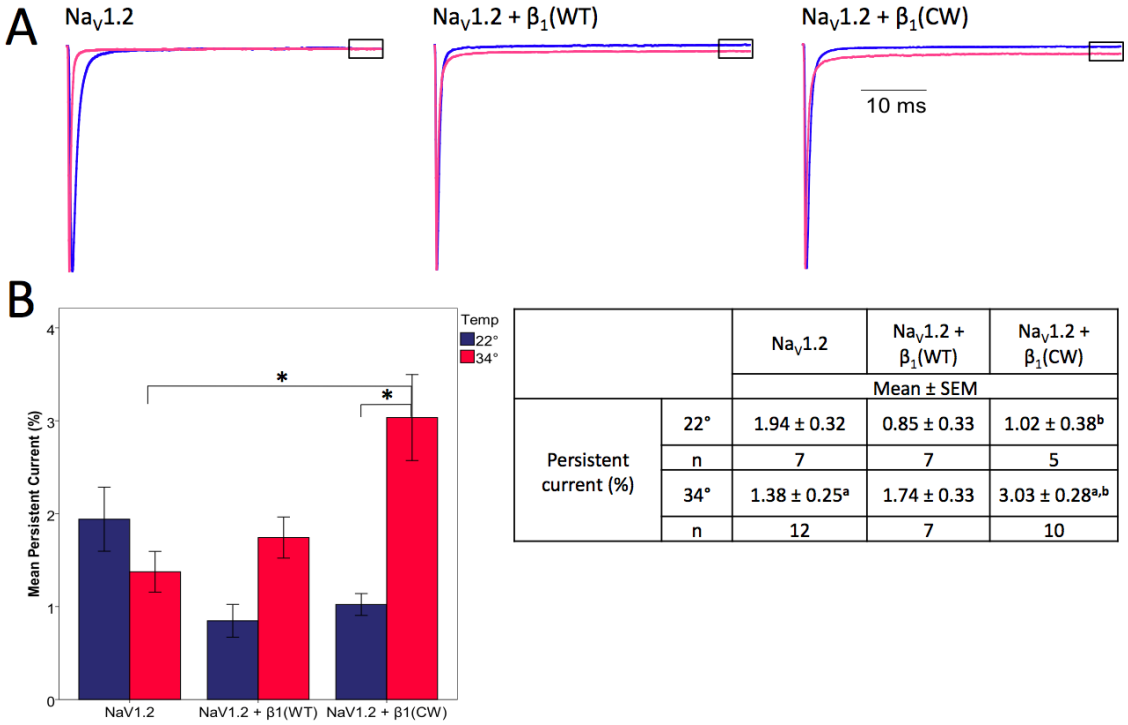

		$Na_V1.2$	$Na_V1.2 + \beta_1(WT)$	$Na_V1.2 + \beta_1(CW)$
		Mean ± SEM		
Persistent current (%)	22°	1.94 ± 0.32	0.85 ± 0.33	1.02 ± 0.38[b]
	n	7	7	5
	34°	1.38 ± 0.25[a]	1.74 ± 0.33	3.03 ± 0.28[a,b]
	n	12	7	10

A) Typical current traces of a 50ms pulse to 0mV at 22°C (blue) and 34°C (pink) of $Na_V1.2$ (left), $Na_V1.2 + \beta_1(WT)$ (middle), and $Na_V1.2 + \beta_1(CW)$ (right). I_{NaP} was measured between 45-50ms (shown in boxed area) and calculated as percent of peak current. Mean I_{NaP} values displayed in the table. Matching superscript letters in the table indicate statistically significant difference at $p<0.05$.
B) Mean I_{NaP} for each subunit at 22°C (blue) and 34°C (red) with error bars of ±1 S.E.M. $Na_V1.2 + \beta_1(CW)$ had significantly greater I_{NaP} at 34°C than $Na_V1.2$ ($p<0.05$). Elevated temperature significantly increased I_{NaP} only in $Na_V1.2 + \beta_1(CW)$ ($p<0.05$). Two-way ANOVA showed a significant interaction term for temperature*subunit ($p<0.05$) indicating that the change in I_{NaP} varies with subunit and temperature.

5.4 Elevated temperature decreases the maximum probability of steady-state SI.

Action potential firing is determined by the fraction of channels available for activation, and long-term channel availability is determined by the proportion of channels in the SI state. To test if the β_1(CW) mutant increases long-term channel availability at elevated temperature, I measured the voltage-dependence of steady-state SI for all subunits at both temperatures. Figure 7A illustrates steady-state SI for all subunits with modified Botzmann fits at 22°C (blue) and 34°C (pink). The maximum probability of SI was derived

from the steady-state plateau of the Boltzmann fit at depolarized voltages. At 22°C, channels displayed relatively complete SI, with less that 10% current remaining after 50s at 0mV. The maximum probability of steady-state SI was significantly decreased at 34°C for all subunits, as illustrated by an increase in steady-state asymptote (Fig 7C, $p<0.05$, and $p<0.01$ for $Na_V1.2+\beta_1$(WT)). The wild-type β_1 demonstrated the greatest increase in asymptote, and was significantly higher at 34°C than $Na_V1.2+\beta_1$(CW) ($p<0.05$). The wild-type β_1 also appeared to have a higher SI asymptote than $Na_V1.2$ and $Na_V1.2 + \beta_1$(CW) at 22°C, however the results were not significant. Neither the $V_{1/2}$ nor slope factor of steady-state SI was affected by temperature or subunit expression (Fig 7B and C).

Figure 7. Steady-state SI.

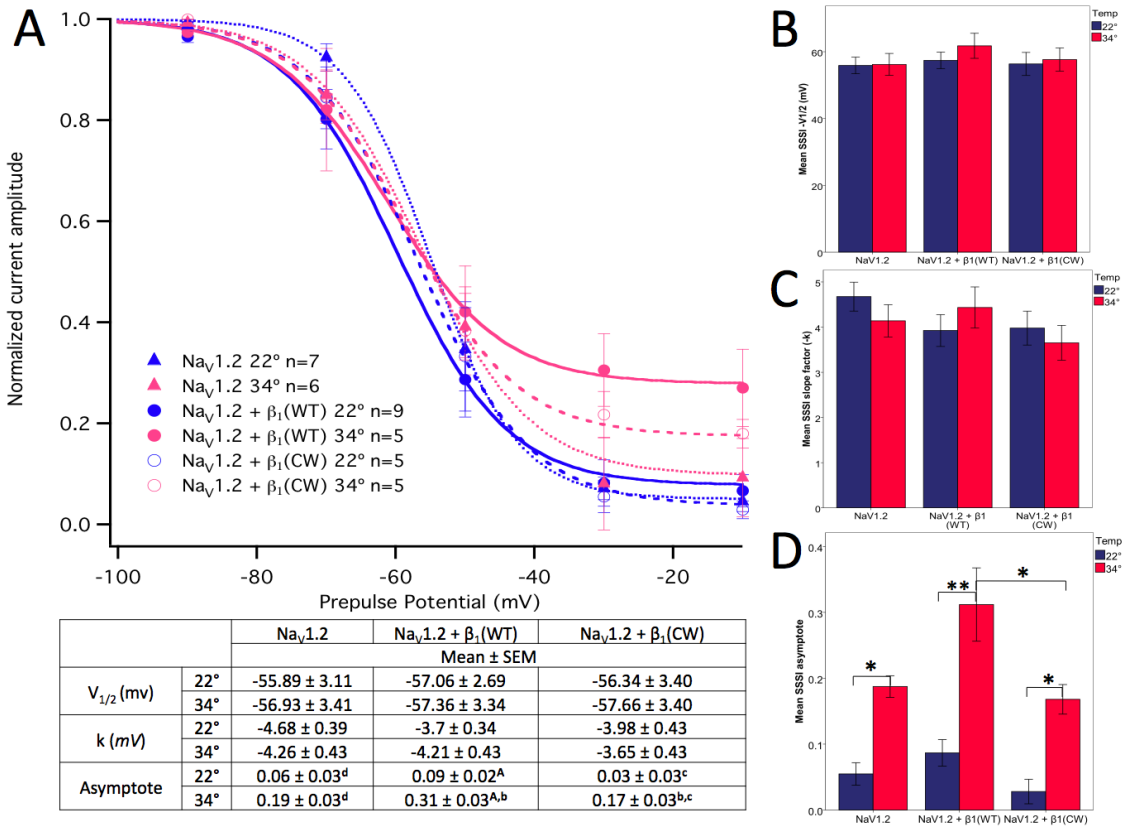

		$Na_V1.2$	$Na_V1.2 + \beta_1$(WT)	$Na_V1.2 + \beta_1$(CW)
		Mean ± SEM		
$V_{1/2}$ (mv)	22°	-55.89 ± 3.11	-57.06 ± 2.69	-56.34 ± 3.40
	34°	-56.93 ± 3.41	-57.36 ± 3.34	-57.66 ± 3.40
k (*mV*)	22°	-4.68 ± 0.39	-3.7 ± 0.34	-3.98 ± 0.43
	34°	-4.26 ± 0.43	-4.21 ± 0.43	-3.65 ± 0.43
Asymptote	22°	0.06 ± 0.03^{d}	0.09 ± 0.02^{A}	0.03 ± 0.03^{c}
	34°	0.19 ± 0.03^{d}	0.31 ± 0.03^{A,b}	0.17 ± 0.03^{b,c}

A) Normalized current amplitude as a function of prepulse potential. Voltage protocol as described in Methods. Mean values of Boltzmann fit are displayed in the table. Matching superscript letters in the table indicate statistically significant difference at $p<0.05$, and capital superscripts indicate $p<0.01$.
B) Mean $V_{1/2}$ values with ±1S.E.M. No statistically significant differences were found.
C) Mean slope factors with ±1S.E.M. No statistically significant differences were found.
D) Mean asymptote values with ± 1S.E.M. The asymptote of SSSI completion increased for all subunits at elevated temperature ($p<0.05$ and $p<0.01$ for $Na_V1.2 + \beta_1$(WT))**.** $Na_V1.2 + \beta_1$(WT) had a significantly higher asymptote value at 34°C than $Na_V1.2 + \beta_1$(CW) ($p<0.05$).

5.5 Temperature differentially affects the fast and slow components of SI onset at +10mV.

To better understand how temperature elevation increases the asymptote of steady-state SI, I measured the rate of SI onset at a membrane potential at which there is a maximum probability SI. Figure 8A illustrates normalized current amplitude as a function

of a +10mV prepulse duration for all subunits with double exponential fits at 22°C (blue) and 34°C (pink). Elevated temperature significantly accelerated the rate of the fast component of SI onset for all subunits as shown by a decrease in the first time constant (τ_1) of the bi-exponential fit (Fig 8B, $p<0.05$). The second time constant (τ_2), on the other hand, was significantly larger for all subunits at 34°C (Fig 8C, $p<0.05$). The average relative amplitude of the slow component of fit was also smaller at 34°C, indicating that a smaller portion of current decay can be attributed to the slow component of SI onset (Supplementary Table 2, $p<0.01$). Figure 8A inset shows prepulse duration on a log scale to illustrate the differential effect of temperature on the fast and slow components of SI onset.

All subunits reached a maximum probability of SI onset after approximately 40s at +10mV, except for $Na_V1.2+\beta_1$(CW), which did not reach an asymptotic value within 64s at 34°C. To account for this difference, I did statistical analysis comparing the average normalized current amplitudes at 64s as well as comparing the asymptote values given by the double exponential fits to the data. There were no differences in statistical conclusions using either method, therefore the term asymptote will be used from now on.

The average asymptote of SI onset was significantly increased for all subunits with elevated temperature (Fig 8D, $p<0.05$). This temperature-induced destabilization of the SI state is in agreement with the results observed for steady-state SI (Fig 7A). The asymptote of $Na_V1.2+\beta_1$(CW), on average, did not significantly differ from $Na_V1.2$, but was significantly lower than $Na_V1.2+\beta_1$(WT) ($p<0.05$), also in agreement with results seen for steady-state SI.

Figure 8. SI onset at +10mV.

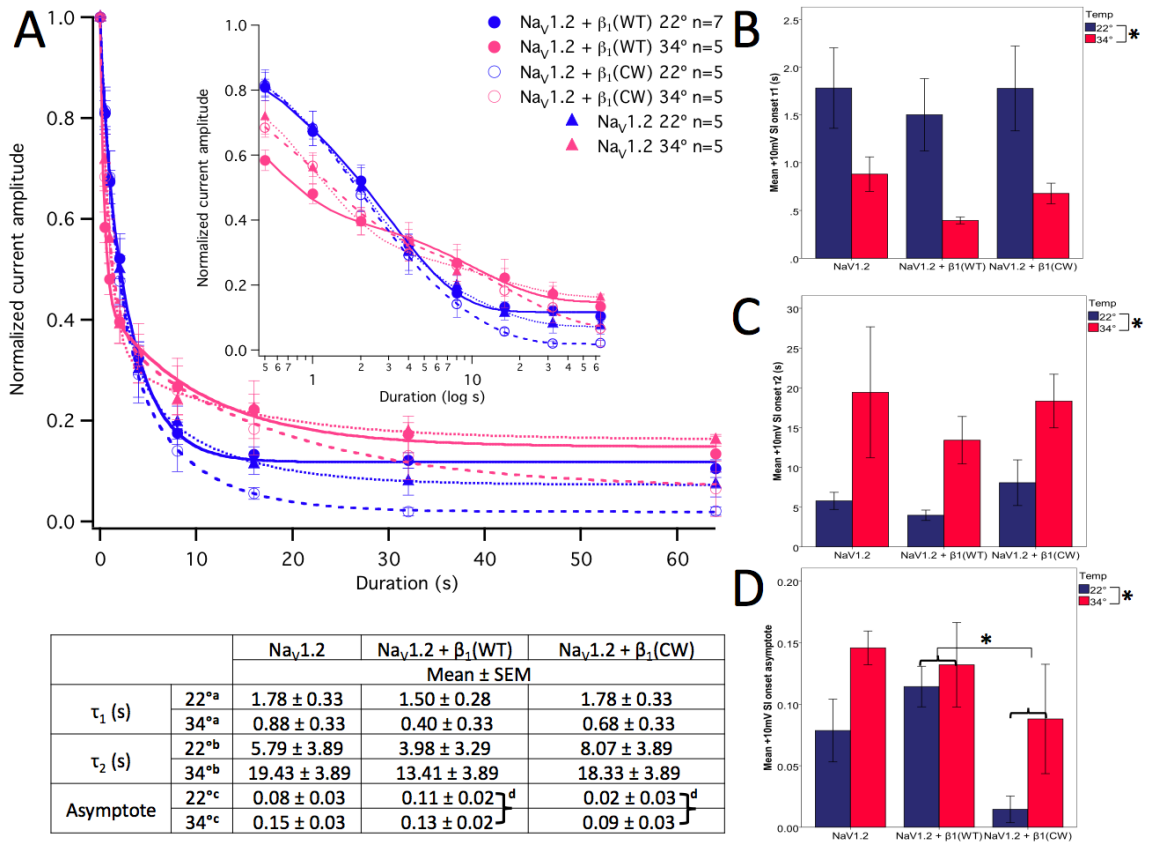

		Na$_V$1.2	Na$_V$1.2 + β$_1$(WT)	Na$_V$1.2 + β$_1$(CW)
		Mean ± SEM		
τ_1 (s)	22°^{a}	1.78 ± 0.33	1.50 ± 0.28	1.78 ± 0.33
	34°^{a}	0.88 ± 0.33	0.40 ± 0.33	0.68 ± 0.33
τ_2 (s)	22°^{b}	5.79 ± 3.89	3.98 ± 3.29	8.07 ± 3.89
	34°^{b}	19.43 ± 3.89	13.41 ± 3.89	18.33 ± 3.89
Asymptote	22°^{c}	0.08 ± 0.03	0.11 ± 0.02^d	0.02 ± 0.03^d
	34°^{c}	0.15 ± 0.03	0.13 ± 0.02	0.09 ± 0.03

A) Normalized current amplitude as a function of prepulse duration. Voltage protocol as described in Methods. Mean values of double exponential fits are displayed in the table. Matching superscript letters in the table indicate statistically significant difference at $p<0.05$. **Inset:** Log time scale of SI onset to illustrate bi-exponential components of fit. **B)** Mean τ_1 values with ± 1S.E.M. At 34°C the averaged τ_1 for all subunits were significantly smaller than at 22°C (1.52s ± 0.2s, 0.65s ± 0.2s respectively; $p<0.01$). **C)** Mean τ_2 values with ± 1S.E.M. The averaged τ_2 were significantly larger at elevated temperature (17.05 ± 2.2s, 5.94s ± 2.1s at 34°C and 22°C respectively; $p<0.01$). **D)** Mean asymptote values with ± 1S.E.M. The asymptote values for all subunits were significantly higher at 34°C than at 22°C (0.069 ± 0.015, 0.12 ± 0.015 respectively; $p<0.05$), and the average asymptote value at both temperatures for Na$_V$1.2 + β$_1$(CW) was significantly lower than for Na$_V$1.2 + β$_1$(WT) (0.052 ± 0.02, 0.12 ± 0.017 respectively; $p<0.05$).

5.6 Neither temperature nor subunit expression significantly affects SI recovery at -90mV.

For a more complete understanding of how subunit expression and temperature affects SI properties, the rate of recovery of SI was also assessed for all subunits at both temperatures. Figure 9A illustrates normalized current amplitude as a function of a -90mV

prepulse duration fit with a double exponential at 22°C (blue) and 34°C (pink). Although not within a physiological voltage range, a membrane potential of -90mV allows for almost maximal recovery from the SI state, with minimal SI onset (see Fig 7A). Recovery duration is plotted on a log scale in Figure 9A inset to highlight the bi-exponential nature of SI recovery. Elevated temperature did not significantly affect either the fast or slow component of SI recovery, or the asymptote value (Fig 9B,C and D). Although expression of the mutant β_1 subunit appeared to accelerate recovery at 34°C compared to $Na_V1.2$ alone or wild-type β_1, the results were not significant.

Figure 9. SI recovery at -90mV.

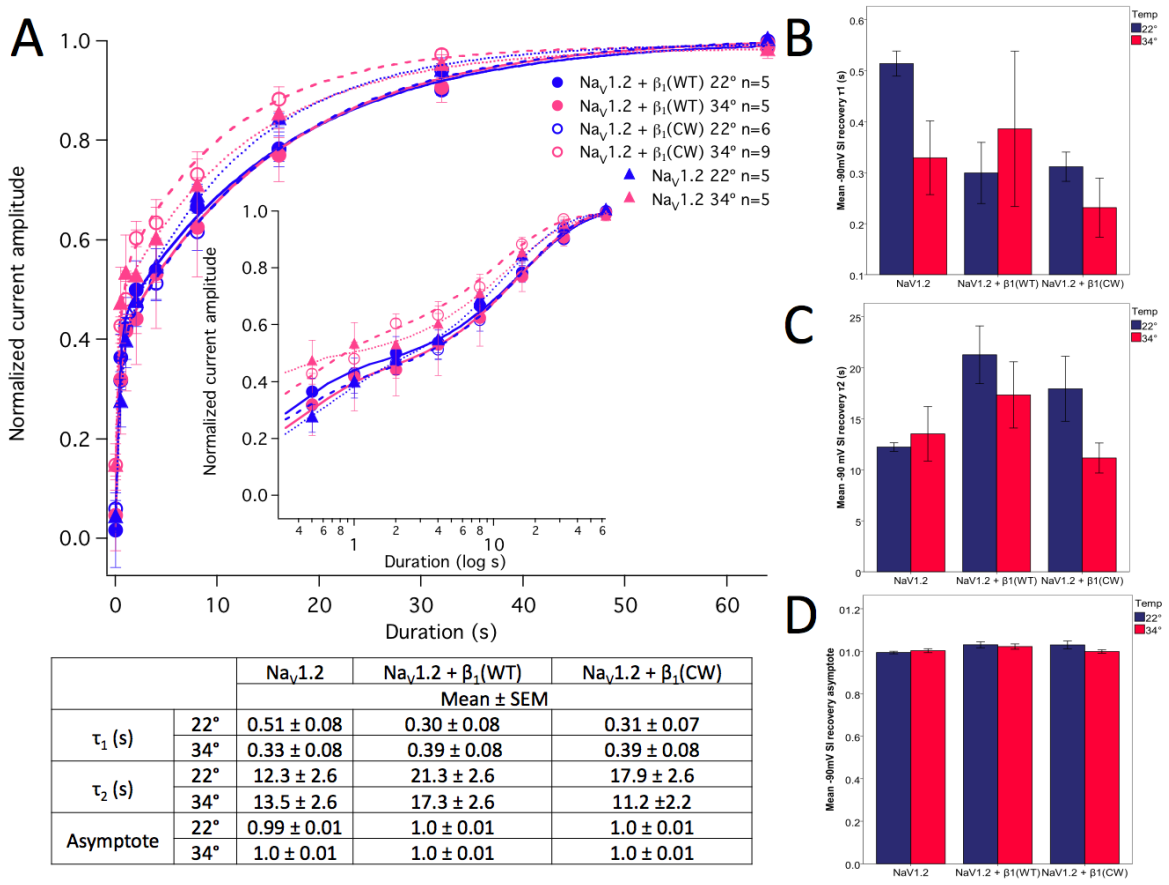

		$Na_V1.2$	$Na_V1.2 + \beta_1$(WT)	$Na_V1.2 + \beta_1$(CW)
		Mean ± SEM		
τ_1 (s)	22°	0.51 ± 0.08	0.30 ± 0.08	0.31 ± 0.07
	34°	0.33 ± 0.08	0.39 ± 0.08	0.39 ± 0.08
τ_2 (s)	22°	12.3 ± 2.6	21.3 ± 2.6	17.9 ± 2.6
	34°	13.5 ± 2.6	17.3 ± 2.6	11.2 ±2.2
Asymptote	22°	0.99 ± 0.01	1.0 ± 0.01	1.0 ± 0.01
	34°	1.0 ± 0.01	1.0 ± 0.01	1.0 ± 0.01

A) Normalized current amplitude as a function of recovery pulse duration**.** Voltage protocol as described in Methods. Mean values of double-exponential fit are displayed in the table. Matching superscript letters in the table indicate statistically significant difference at $p<0.05$. **Inset:** Log time scale of SI recovery to illustrate bi-exponential components of fit.
B) Mean τ_1 values with ± 1S.E.M. No statistically significant differences were found.
C) Mean τ_2 values with ± 1S.E.M. No statistically significant differences were found.
D) Mean asymptote values with ± 1S.E.M. No statistically significant differences were found.

5.7 $Na_V1.2 + \beta_1$(CW) reduces UDI at elevated temperatures.

Use-dependent inactivation is an important determinant of channel availability in high frequency firing neurons, therefore it is important to understand how an FS-causing mutation affects this channel property, especially at elevated temperature. Figure 10A illustrates normalized current amplitude as a function of a 50Hz pulse train from -60mV to

0mV for $Na_V1.2+\beta_1$(CW) (left), $Na_V1.2+\beta_1$(WT) (top right), and $Na_V1.2$ (bottom right) at 22°C (blue) and 34°C (pink). Current decay was fit with a double exponential function to 15s. All subunits showed relatively robust UDI at 22°C (~70% decrease from maximal current) with a current decay plateau at about 15s. Elevating the temperature greatly increased the fast component (τ_1) of UDI (up to 18 fold increase) for all subunits, with an average Q_{10} of 8.9 (Fig 10B, $p<0.05$). The average relative amplitude of the fast component of fit also decreased with elevated temperature (Supplementary Table 2, $p<0.01$). Figure 10A inset shows an expanded view of UDI from 0-1s to illustrate the difference in τ_1 at 22°C and 34°C. At 22°C, channels rapidly accumulate into the inactivated state (within the first 3 depolarizing pulses), resulting in a steep slope of the first component of fit. Raising the temperature to 34°C removes the initial rapid inactivation, resulting in a much shallower slope of the first component of fit and larger τ_1. The slow component (τ_2) of inactivation was relatively unaffected by temperature (Fig 10C), however the average relative amplitude of the slow component of fit decreased with elevated temperature (Supplementary Table 2, $p<0.01$). Raising the temperature to 34°C resulted in a 120% increase in the asymptote (measured at 15s) for $Na_V1.2+\beta_1$(CW) ($p<0.01$) and a 92% increase for $Na_V1.2$ ($p<0.05$) while the asymptote for $Na_V1.2+\beta_1$(WT) remained unaffected by temperature (Fig 10D).

Figure 10. Use-dependent inactivation.

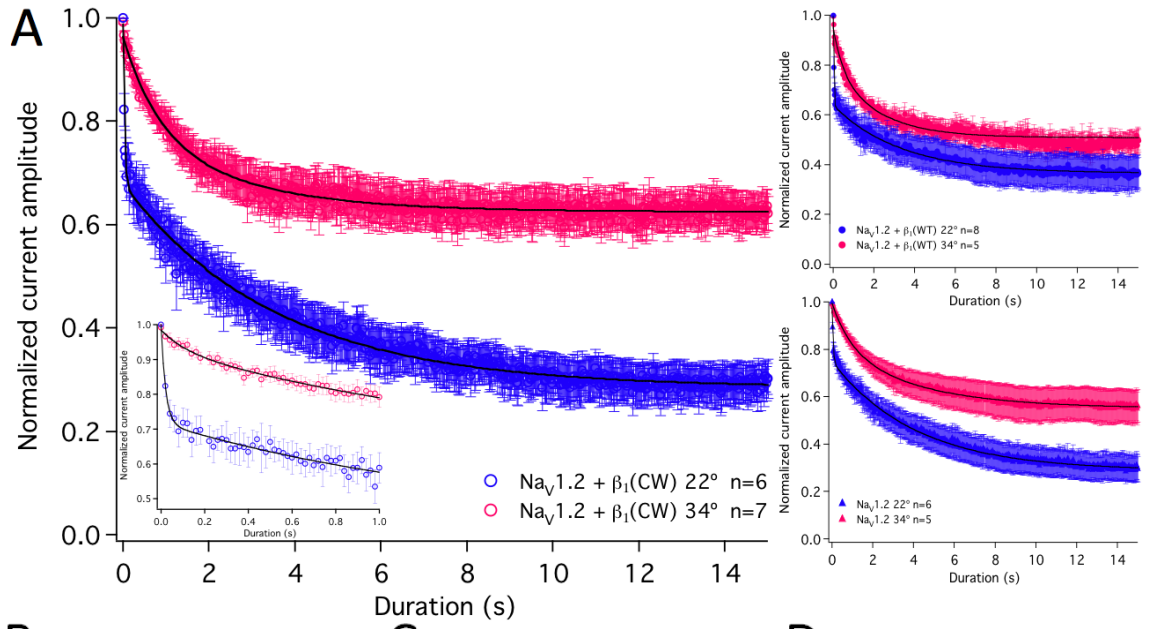

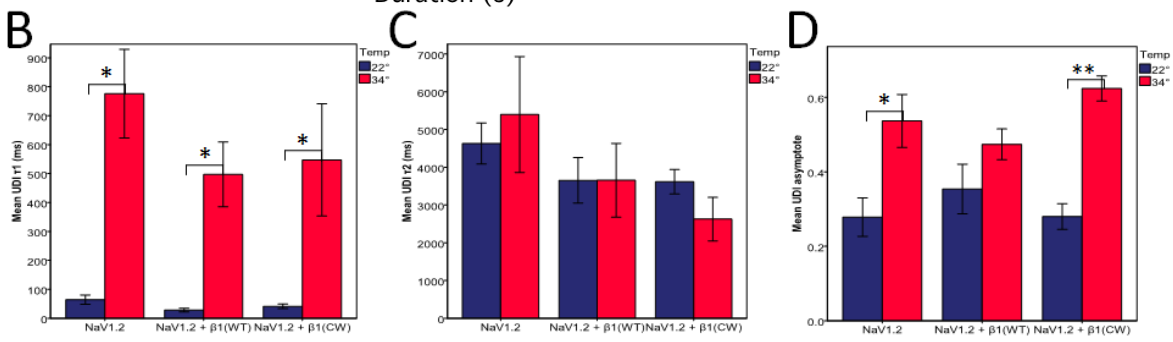

		$Na_V1.2$	$Na_V1.2 + \beta_1$(WT)	$Na_V1.2 + \beta_1$(CW)
		Mean ± SEM		
τ_1 (ms)	22°	64.0 ± 111.4[c]	27.8 ± 96.5[e]	41.2 ± 111.4[d]
	34°	776.1 ± 122.0[c]	496.8 ± 122.0[e]	546.9 ± 103.1[d]
τ_2 (ms)	22°	4629 ± 777	3652 ± 673	3615 ± 777
	34°	5397 ± 852	3656 ± 851	2624 ± 719
Asymptote	22°	0.28 ± 0.05[b]	0.35 ± 0.05	0.28 ± 0.05[A]
	34°	0.54 ± 0.06[b]	0.47 ± 0.06	0.62 ± 0.025[A]

A) Normalized current amplitude as a function of pulse train duration for $Na_V1.2 + \beta_1$(CW) (left), $Na_V1.2 + \beta_1$(WT) (top right), and $Na_V1.2$ (bottom right). Voltage protocol as described in Methods. Mean values of double exponential fits are displayed in the table. Matching superscript letters in the table indicate statistically significant difference at $p<0.05$, and capital superscripts indicate $p<0.01$. Inset illustrates UDI from 0-1s to highlight the differences in the fast component of decay between the two temperatures ($Na_V1.2 + \beta_1$(CW) shown). Channels rapidly inactivate (within the first 100ms) at 22°C, and are much slower to inactivate at 34°C. **B)** Mean τ_1 values with ± 1S.E.M. Elevated temperature significantly increased τ_1 for all subunits ($p<0.05$). **C)** Mean τ_2 values with ± 1S.E.M. No statistically significant differences were found. **D)** Mean asymptote values with ± 1S.E.M. Elevated temperature decreased UDI as shown by an increased UDI asymptote for $Na_V1.2 + \beta_1$(CW) ($p<0.01$) and $Na_V1.2$ ($p<0.05$) but not for $Na_V1.2 + \beta_1$(WT). $Na_V1.2 + \beta_1$(CW) had a greater temperature dependent increase in UDI asymptote than did $Na_V1.2$ (120% increase for $Na_V1.2 + \beta_1$(CW) and 92% increase for $Na_V1.2$).

5.8 Elevated temperature speeds FI recovery more than FI onset.

To better understand the mechanism of the temperature-induced increase in the fast component of UDI, I compared the temperature sensitivity of the rate of FI onset at 0mV (membrane potential of UDI depolarizing pulse) to the rate of recovery from FI at -60mV (membrane potential of UDI interpulse).

Open-state FI was measured by a single exponential fit to macroscopic current decay from -20mV to 20mV, and the derived τ values were plotted in Figure 11 for all subunits at 22°C (blue) and 34°C (pink). Elevated temperature significantly decreased the τ of open-state FI for all subunits across all measured voltage ranges ($p<0.05$). The magnitude of change in τ at 0mV was not statistically different among subunits and yielded an average Q_{10} of 2. Temperature elevation revealed a subunit effect at more hyperpolarized voltages, however, where at -20mV $Na_V1.2+\beta_1$(CW) had a significantly larger τ value compared to $Na_V1.2+\beta_1$(WT) (Fig 11, $p<0.05$). The decreased rate of current decay at -20mV in $Na_V1.2+\beta_1$(WT) at 34°C can be observed in Fig 11 inset, which shows current traces for each subunit at 22°C (blue) and 34°C (red), with bolded traces at -20mV.

The rate of FI recovery was also increased by elevated temperature, as shown in Figure 11A where normalized current amplitude is plotted as a function of a -60mV recovery pulse duration. Recovery was best fit with a double exponential equation, as reported previously[60, 109, 110]. A double exponential fit to recovery is partially due to an extended recovery pulse duration (up to 1s), which includes some recovery from intermediate inactivation. The log plot of recovery shows two slope components, suggesting recovery up to 1s is a multistep process (Supplementary Fig.1). Elevated temperature increased the fast component of recovery for all subunits, as shown by a significant

decrease in τ_1 (Fig 12B, $p<0.05$), but did not affect the slow component (Fig 12C). Because the τ_1 of FI recovery did not significantly differ between subunits, an average Q_{10} was calculated for all subunits, yielding a value of 2.8, 1.4 times greater than the Q_{10} of FI onset. This shows that increasing temperature accelerates the rate of FI recovery to a greater extent than the rate of FI onset.

Because the UDI protocol had only a 15ms interpulse duration at -60mV, I also assessed recovery from FI within this time frame. Figure 12A inset shows FI recovery fit with a double-exponential equation up to 16ms. $Na_V1.2$ and $Na_V1.2 + \beta_1$(CW) had significantly higher normalized current amplitudes (indicating a greater proportion of recovery) at 34°C than at 22°C for each recovery duration up to 16ms ($p<0.001$). $Na_V1.2 + \beta_1$(CW) also showed significantly greater proportion of recovery at 34°C than $Na_V1.2 + \beta_1$(WT) (asterisks in Figure 12A inset, $p<0.01$). The normalized current amplitude of $Na_V1.2 + \beta_1$(WT) did not significantly differ between temperatures within the measured time frame.

Figure 11. Open-state FI.

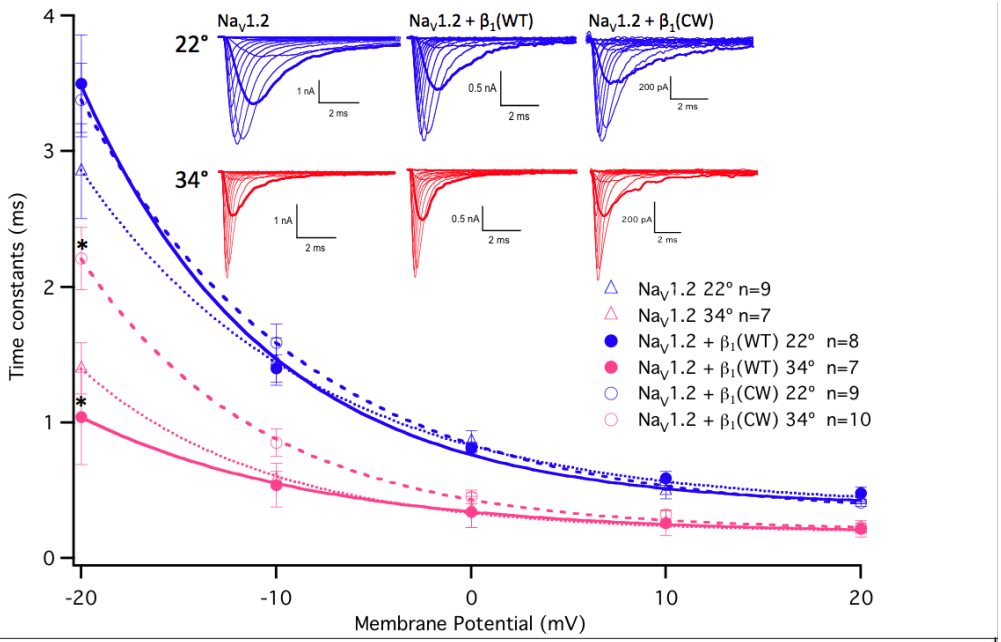

		Mean ± SEM														
		Na$_V$1.2					Na$_V$1.2 + β$_1$(WT)					Na$_V$1.2 + β$_1$(CW)				
Membrane potential (mV)		-20	-10	0	10	20	-20	-10	0	10	20	-20	-10	0	10	20
τ (ms)	22°	2.60^{a} ± 0.27	1.39^{b} ± 0.18	0.82^{c} ± 0.07	0.58^{d} ± 0.05	0.47^{e} ± 0.05	3.55^{f} ± 0.36	1.41^{g} ± 0.10	0.81^{h} ± 0.04	0.59^{i} ± 0.05	0.49^{j} ± 0.05	3.39^{k} ± 0.28	1.59^{l} ± 0.14	0.82^{m} ± 0.04	0.55^{n} ± 0.02	0.42^{o} ± 0.02
	34°	1.40^{a} ± 0.20	0.5^{b} ± 0.06	0.36^{c} ± 0.03	0.26^{d} ± 0.03	0.21^{e} ± 0.02	1.04^{f,p} ± 0.13	0.54^{g} ± 0.06	0.34^{h} ± 0.04	0.27^{i} ± 0.04	0.22^{j} ± 0.02	2.21^{k,p} ± 0.23	0.87^{l} ± 0.11	0.48^{m} ± 0.06	0.33^{n} ± 0.03	0.24^{o} ± 0.03

Open-state FI time constants were derived from single exponential fits to macroscopic current decay. Voltage protocol as described in Methods. Mean time constants of current decay are displayed in the table. Matching superscript letters in the table indicate statistically significant difference at $p<0.05$. Increased temperature decreased the time constant of open state FI for all subunits, however the rate of FI in Na$_V$1.2 + β$_1$(CW) is slowed at 34°C compared to Na$_V$1.2 + β$_1$(WT) (* indicates $p<0.05$). **Inset:** Representative current traces at 22°C (peak current at +10mV) and 34°C (peak current at 0mV) with bolded traces at -20mV.

Figure 12. FI recovery at -60mV.

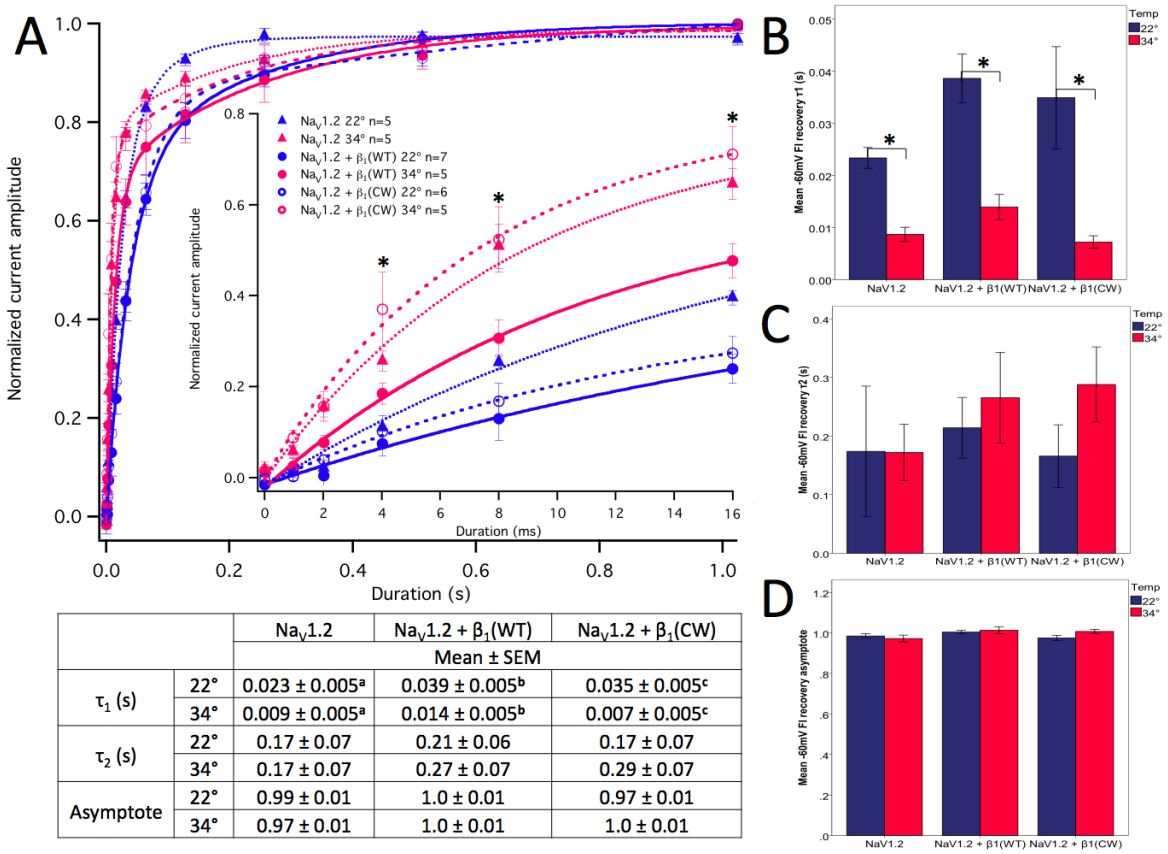

		$Na_V1.2$	$Na_V1.2 + \beta_1(WT)$	$Na_V1.2 + \beta_1(CW)$
		Mean ± SEM		
τ_1 (s)	22°	0.023 ± 0.005[a]	0.039 ± 0.005[b]	0.035 ± 0.005[c]
	34°	0.009 ± 0.005[a]	0.014 ± 0.005[b]	0.007 ± 0.005[c]
τ_2 (s)	22°	0.17 ± 0.07	0.21 ± 0.06	0.17 ± 0.07
	34°	0.17 ± 0.07	0.27 ± 0.07	0.29 ± 0.07
Asymptote	22°	0.99 ± 0.01	1.0 ± 0.01	0.97 ± 0.01
	34°	0.97 ± 0.01	1.0 ± 0.01	1.0 ± 0.01

Figure 10. Fast inactivation recovery at -60mV. A) Normalized current amplitude as a function of recovery pulse duration. Mean values of double-exponential fit are displayed in the table. Matching superscript letters in the table indicate statistically significant difference at $p<0.05$. **Inset:** Recovery duration shown up to 16ms. $Na_V1.2$ and $Na_V1.2 + \beta_1(CW)$ had significantly higher normalized current amplitudes at 34°C than at 22°C for all recovery durations up to 16ms ($p<0.001$). Asterisks indicate significant difference in normalized current amplitude at 34°C between $Na_V1.2 + \beta_1(WT)$ and $Na_V1.2 + \beta_1(CW)$ ($p<0.01$). **B)** Mean τ_1 values with ± 1S.E.M. Temperature increased the fast component of FI recovery, τ_1, for all subunits ($p<0.05$). **C)** Mean τ_2 values with ± 1S.E.M. No statistically significant differences were found. **D)** Mean asymptote values with ± 1S.E.M. No statistically significant differences were found.

5.9 Summary

Results from the present study support the hypothesis that the β_1(CW) mutation alters Na_V channel thermosensitivity compared to the wild-type subunit. Table 1. lists the respective changes to $Na_V1.2$ channel properties in response to elevated temperature with co-expression of the wild-type and mutant subunits. Co-expression of β_1(CW) results in increased channel excitability with elevated temperature compared to β_1(WT). These results are consistent with mutationally induced neuronal hyperexcitability and increased susceptibility to FS.

Table 1. Summary of results

	Effect of elevated temperature	
	$Na_V1.2 + \beta_1$(CW)	**$Na_V1.2 + \beta_1$(WT)**
Persistent current	↑	no change
Window current	↑	no change
Use-dependent inactivation	↓	no change
Rate of FI onset	↓ compared to β_1(WT)	↑
Rate of FI recovery	↑ compared to β_1(WT)	↑

6: DISCUSSION

Previous studies investigating the mechanism of FS show that elevated temperature increases neuronal excitability[7, 84, 85] and that this is partly due to an increased excitability of Na_V channels[7, 8, 63]. Most studies on the functional consequences of mutations causing GEFS+, on the other hand, have been conducted at room temperature. Such room temperature observations suggest that the seizure causing mechanism of the β_1 subunit mutation C121W, for example, is a decrease or loss of β_1 function resulting in increased Na_V channel excitability[30, 32, 92, 111]. A single study did investigate the effect of temperature on β_1(CW), and showed that neurons expressing the mutant subunit displayed an increased temperature-dependent excitability compared to wild-type neurons[7]. These results coincide well with the paroxysmal phenotype of GEFS+, as the functional effect of the seizure causing mutation was enhanced at elevated temperature. Because the methodology of the latter study involved action potential recordings from neurons expressing the β_1(CW) mutation, the mechanism of the increased temperature sensitivity at the channel level remained undescribed.

This study provides novel insights into the FS mechanism at the molecular level by measuring voltage-dependent properties of the neuronal $Na_V1.2$ α subunit alone, as well as with β_1(WT) or β_1(CW) at both 22ºC and 34ºC. I report that the β_1(WT) subunit has a thermoprotective role in the regulation of channel excitability, and link the previous reports of temperature-dependent increases in excitability of $Na_V1.2$ and $Na_V1.2$+β_1(CW) to a loss of this protective function.

In the absence of the β_1(WT) subunit, elevating the temperature resulted in a destabilization of inactivated states. Specifically, temperature decreased UDI, reduced the maximum probability of SI, increased window current, depolarized the voltage-dependence of FI and accelerated FI recovery. Elevated temperature also increased the open probability of channels by hyperpolarizing the voltage-dependence of activation. In the presence of β_1(WT), $Na_V1.2$ channels no longer displayed an increase in window current or decreased UDI at elevated temperature.

In comparison, co-expression with the β_1(CW) mutation resulted in slowed FI onset, increased FI recovery, decreased UDI, and increased window current and persistent current at 34ºC. Because co-expression of β_1(CW) also showed subtle differences compared to the $Na_V1.2$ α subunit alone, such as increased I_{NaP} and left-shifted stead-state FI, this suggests that β_1(CW) does not result in a complete loss of β_1 function. The reduced thermoprotection as a result of this mutation, however, is a likely contributor to the FS mechanism.

6.1 The β_1(CW) mutation results in moderate alterations to β_1 subunit function at room temperature.

Specific results of the functional effects of β_1(CW) and β_1(WT) vary across laboratories, expression systems, and Na_V channel isoforms. In general, however, this study supports previous findings that, at room temperature, β_1(CW) impairs β_1(WT) modulation of Na_V channel function. My experiments using CHO cells stably expressing $Na_V1.2$ show that, at 22°C, β_1(CW) impairs β_1(WT) modulation of steady-state FI.

Co-expression with either the wild-type or mutant subunit resulted in a lower slope factor of the Boltzmann fit to steady-state FI compared to $Na_V1.2$ alone. This indicates that in the presence of a β_1 subunit, there is a decreased movement of charge across the electric

field during the transition into the FI state. Steric interactions between the extracellular segment of the β_1 subunit and the DI, DIV S5-S6 linker may be responsible for this observation.

Unlike the slope factor, the voltage-dependence,$V_{1/2}$, of FI was differentially affected by β_1(WT) and β_1(CW). Expression of the β_1(WT) subunit resulted in a large depolarizing shift in the $V_{1/2}$ of FI, while the β_1(CW) mutation showed reduced modulation of FI. These observations are comparable to previous reports on the effects of β_1(WT) and β_1(CW) on FI[21, 32, 33, 96] and support the role of the β_1(WT) subunit as a damper of channel excitability. The reduced modulation of FI with the mutant subunit indicates that, at RMP (-60mV), there would be about 20% more channels available for activation when $Na_V1.2$ is associated with β_1(CW) compared to β_1(WT), consistent with a hyperexcitable phenotype.

While both the β_1(WT) and β_1(CW) depolarized the $V_{1/2}$ of FI compared to $Na_V1.2$, neither subunit had a significant effect on SI at room temperature. This is contrary to previous reports of the β_1 subunit depolarizing the $V_{1/2}$ of steady-state SI when co-expressed with $Na_V1.2$ and $Na_V1.4$ in HEK cells[33, 37]. Elevating the temperature, however, revealed a β_1 subunit induced destabilization of the SI state, results which are discussed in further detail in sections 6.2.4 through 6.2.6.

6.2 Thermosensitivity of $Na_V1.2$, $Na_V1.2$ + β_1(WT) and $Na_V1.2$ + β_1(CW)

In accordance with previous studies on the consequences of temperature elevation on channel function, I show a general trend of increased channel excitability at 34°C compared to 22°C. This increased excitability is modulated by the expression of the β_1 subunit.

6.2.1 Voltage-dependence of activation

A hyperpolarizing shift in, and elevated slope factor of, the voltage-dependence of activation with temperature elevation has been shown previously[8,59] (but see[9, 10, 55-58] where no shift is observed). To predict how this temperature induced change might affect neuronal excitability during febrile states; I used the average Q_{10} values to extrapolate the $V_{1/2}$ of activation to a range of physiological temperatures. Assuming that the Q_{10} value is constant across temperatures, I predict a 1.2mV hyperpolarizing shift in the $V_{1/2}$ of activation from 37°C to 41°C. Although this effect is pro-excitatory, as channel opening will occur with less of a depolarizing stimulus, the magnitude of the predicted change is a relatively small. It is therefore likely that temperature induced changes to channel activation play only a minor role in neuronal excitability.

6.2.2 Voltage-dependence of steady-state FI

Previous reports on the effect of temperature on FI are also varied, showing either no shift[13, 59, 112] a hyperpolarizing shift[8] or a depolarizing shift[12, 60]. The results from this study agree with the latter, that temperature increases channel excitability by depolarizing the $V_{1/2}$ of FI. Using the average Q_{10} value for the change in $V_{1/2}$ of FI, I predict a 1.4 mV depolarizing shift with a temperature elevation from 37ºC to 41ºC. This change is quite small, as it would result in less than a 1% increase in channel availability at any given voltage. This suggests that, similar to channel activation, temperature dependent changes to FI play only a minute role in excitability.

6.2.3 Window current and I_{NaP}

Although the effects of temperature on activation and inactivation were small, the collective left shift in activation and right shift in FI produced an increased area of window current in $Na_V1.2$ and $Na_V1.2 + \beta_1$(CW). The increased area of window current at 34°C indicates that a larger proportion of channels activate but fail to fast-inactivate throughout the voltage range of -60 to 0 mV. Window current results in a low-level depolarizing current that increases neuronal excitability if it occurs across a voltage range that includes the RMP. Although this study shows that window current occurs only at non-resting membrane potentials, voltage-dependent properties recorded from CHO cells are approximately 15 mV right-shifted compared to measurements from intact neurons[109]. Shifting the relative range of window current 15 mV to the left then, indicates that at elevated temperature there a substantial level of non-inactivating current that occurs during resting membrane potentials. No increase in window current was observed with the co-expression of the β_1(WT) subunit however, suggesting that β_1 is thermoprotective against increased neuronal excitability. The β_1(CW) mutant in comparison, further contributed to depolarization of the membrane potential elevated temperatures by increasing I_{NaP}.

The level of I_{NaP} did not differ among subunits at 22°C (also shown previously[96]), but increasing the temperature to 34°C increased the amount of I_{NaP} in $Na_V1.2 + \beta_1$(CW) and not in $Na_V1.2$ or $Na_V1.2 + \beta_1$(WT). The mechanism of this increased I_{NaP} is unclear, as the voltage at which I_{NaP} was measured did not overlap with the voltage range of window current, and the rate of FI-onset did not significantly differ between subunits at 0 mV. Measuring I_{NaP} across a range of voltages might reveal more of the I_{NaP} mechanism. Nevertheless, increased I_{NaP} is another example of how the functional effect of the β_1(CW)

mutation is revealed at elevated temperature, and suggests that β_1(CW) modulates $Na_V1.2$ differently than β_1(WT). The increased I_{NaP} combined with increased window current likely plays a role in heightening FS susceptibility of patients harbouring the β_1(CW) mutation. The small portion of non-inactivating current present when $Na_V1.2$ is co-expressed with β_1(CW) would depolarize the neuronal RMP, bringing the membrane closer to action potential threshold. Such augmented membrane potentials can also predispose neurons to repetitive firing[14].

6.2.4 Voltage-dependence of steady-state SI

No differences were observed in the $V_{1/2}$ of SI between the two temperatures, contrary to some previous studies regarding the temperature sensitivity of SI. Loose-patch recordings on rat IIb muscle fibres show a depolarizing shift in the $V_{1/2}$ of SI with temperature elevation[9]. Similar results are observed using whole-cell patch clamp experiments on HEK cells expressing $Na_V1.4$[12] (however another study in HEK cells expressing $Na_V1.4$ shows no difference in $V_{1/2}$ with temperature[13]). Differences in methodology could account for some observed differences, as the large amount of leak current present in loose-patch recordings has the potential to shift the voltage-dependent properties compared to recordings using a giga-ohm seal. Different Na_V α subunit isoforms also have slightly different SI characteristics, therefore results from this study are not directly comparable to those using $Na_V1.4$ or others[17, 113].

Unlike the $V_{1/2}$ of SI, the maximum probability of steady-state SI was substantially reduced at elevated temperature for all subunits. A decreased probability of entry into the SI state is a pro-excitatory change, as there would be a larger fraction of channels available for activation even after sustained or repetitive depolarizations. Interestingly, $Na_V1.2$ + β_1(WT)

showed the lowest maximum probability of SI at 34°C, contrary to most observations from this study which suggest that β_1(WT) is thermoprotective against temperature-induced excitability. The destabilization of the SI state with co-expression of the β_1(WT) subunit agrees with previous research[33, 37], however, a decreased maximum probability of SI with elevated temperature is a unique observation from this study. The lesser destabilization of SI with the co-expression of β_1(CW) is not surprising, as the CW mutation disrupts the extracellular Ig-like fold, and this region is thought to interact with the p-loop of the α subunit to modulate SI[17]. An increased probability of SI with β_1(CW) compared to β_1(WT) seems counterintuitive in regards to seizure genesis, but current-clamp recordings from neurons lacking β_1(WT) or expressing β_1(CW) clearly show increased excitability[39, 109]. The precise link between stabilization of SI and an increased susceptibility to epileptic discharge has yet to be determined.

6.2.5 Onset and recovery of SI

Temperature altered SI onset in a similar manner to steady-state SI. The maximum probability of onset was reduced for all subunits, with the largest temperature-dependent destabilization observed when $Na_V1.2$ was co-expressed with β_1(WT). Again, the β_1(CW) mutation showed a reduced modulation of SI, an effect which was exaggerated at elevated temperatures.

Interestingly, temperature differentially affected the fast and the slow components of SI onset for all subunits, accelerating the fast component and slowing the slow component. This implies that with elevated temperature, channels are quicker to initiate conformational changes towards the development of SI, but slower to complete the final stages of the SI process. Because SI is thought to take place via conformational changes to

the channel extracellular pore, the increased kinetic energy of sodium ions near or in the pore might hinder completion of these conformational changes, similar to the manner in which increased extracellular sodium concentration hinders SI completion[114]. This slowed secondary component could explain the decreased probability of steady-state SI and SI onset at elevated temperatures. Further studies could investigate isoform-dependent temperature modulation. Differences in flexibility and motility of the p-loop region are thought to contribute to isoform dependent differences in SI properties[17], therefore the increased membrane fluidity and protein motility due to elevated temperature may differentially affect the SI process.

Unlike SI onset, recovery from the SI state was relatively unaffected by temperature, implying that channels that enter the SI state at 34°C recover at the same rate as at 22°C. The differential temperature sensitivity of onset and recovery suggests that recovery of SI may not be a simple reversal of SI onset, but could involve independent conformational changes that are not affected by temperature or expression of β_1 subunits. Measuring the enthalpic change involved during each transition would help clarify the existence of different conformations between SI onset and SI recovery; however, measurements at a minimum of three temperatures are required for such analysis. Multiple crystal structure images of the Na_V channel in each state would further help clarify this issue, but the crystal structure of a mammalian Na_V channel has yet to be determined. There is evidence to suggest however, that the conformational changes involved in SI onset differ from those of SI recovery. Fluorescent probing of S4 voltage sensors in $Na_V1.4$ by Goldstein *et. al*[120] suggests that SI onset is mainly determined by transitions of the S4 segments in DI and DII, while the S4 of DIII is involved in SI recovery. Furthermore, ion-pair interactions observed

in the bacterial Na_V channel NaChBac predict the S4 sensors to adopt a transient, high energy 3_{10}-helical conformation during the transition from resting to activated[121]. A transient 3_{10}-helical transition from a resting α-helical conformation is further supported by histidine scanning of S4 homologues from a voltage-sensitive phosphatase[115]. These observations coincide well with the observation that SI onset (presumably a higher energy transition of the S4 segments) is more temperature sensitive than SI recovery. Any further speculations regarding conformational changes of Na_V channel segments are outside the scope of this study.

6.2.6 Use-dependent inactivation, and onset and recovery of FI.

All subunits displayed relatively robust UDI at 22°C, showing about 70% current reduction after a sequence of depolarizing pulses. Previous studies co-expressing β_1(CW) with $Na_V1.3$ show a reduced UDI relative to β_1(WT)[96], however this study shows that the reduced UDI is only apparent at elevated temperatures. The reduction in UDI seen in $Na_V1.2$ and $Na_V1.2$ + β_1(CW) can be attributed to the decreased maximum probability of SI at 34°C (as observed during steady-state and SI onset protocols). But because $Na_V1.2$ + β_1(WT) had the lowest maximum probability of SI at 34°C, it is difficult to explain how in this instance, the β_1(WT) subunit prevents a temperature-induced decrease in UDI. Observations from steady-state SI and onset protocols would predict a smaller reduction in current amplitude for β_1(WT) compared to $Na_V1.2$ and $Na_V1.2$ + β_1(CW) at 34°C.

Because UDI reflects a combination of FI, intermediate inactivation, and SI, any temperature-dependent changes to intermediate or FI could also influence current decay. Although intermediate inactivation in isolation was not investigated, experiments in $Na_V1.5$ show that elevated temperature enhances intermediate inactivation[116]. Observations from

this study also allude to an increased intermediate inactivation with elevated temperature. At 34°C, a more pronounced secondary slope component was observed in the log plot of FI recovery, reflecting a greater proportion of channels recovering from intermediate inactivation compared to 22ºC. Assessment of how the β_1 subunit modulates intermediate inactivation in neuronal Na_V channels could further explain the differences observed in UDI among the subunits.

Although the role of intermediate inactivation is unclear, variances in FI properties can account for the majority of the observed differences in the initial current decay between the two temperatures. The first component of FI recovery, but not the second, was significantly accelerated at 34°C (similar to results seen in $Na_V1.5$[60,117]). At 22°C, the first time constant of recovery was about 30 ms, resulting in incomplete recovery from FI during the 15ms UDI interpulse to -60mV. The incomplete recovery manifests itself as an initially rapid use-dependent current decay as channels enter the FI state in response to the 5ms pulse to 0mV, but do not recover. At 34°C, the rate of recovery increased almost 2 fold, allowing channels to partially recover during the 15ms interpulse. This partial recovery results in a decreased amount of current decay in the initial portion of UDI protocol. The greater acceleration of FI recovery at -60mV compared to FI onset at 0mV could also explain the initial decrease in UDI seen at elevated temperature. Although the rates of FI onset at 0mV did not differ among subunits, the rate of FI onset at -20mV at 34°C was significantly slowed in $Na_V1.2 + \beta_1$(CW). This suggests that the mutation contributes to increased channel availability with elevated temperature at more hyperpolarized voltages. The mutant β_1(CW) also had an accelerated rate of FI recovery at 34°C, resulting in a decreased amount of current decay with successive depolarizations. This difference

contributes to the relative divergence in maximum current decay between the mutant and wild-type subunits.

Because β_1(WT) prevents a temperature-induced decrease in UDI, the wild-type subunit presumably plays an important neuroprotective role during febrile states. Heat alone can increase the frequency of AP firing[7, 8], therefore the activity-dependent reduction in current amplitude with co-expression of β_1(WT) is protective against sustained, high frequency AP firing. The loss of this function, as in the case of β_1(CW), results in a greater proportion of channels available for activation at elevated temperature, thereby increasing neuronal excitability. If one assumes that the decrease in UDI seen in $Na_V1.2$ + β_1(CW) varies linearly with temperature, then extrapolating these changes to reflect an increase from 37°C to 41°C predicts a 25% decrease in UDI. This is quite a substantial decrease in current decay, which would then increase channel availability at febrile temperatures. Increased channel availability with expression of the β_1(CW) mutant is also seen from AP recordings from CW mice at 22°C and 34°C[7]. The UDI results from this study can attribute the comparatively large increase in AP firing frequency of CW mice at 34° to the loss of the thermoprotective role of the β_1(WT) subunit.

7: CONCLUSIONS

Although it is clear that β_1(CW) increases channel excitability at elevated temperatures, the mechanism of action *in situ* is still speculative. Co-immunipreciptation experiments in CHO cells shows that β_1(CW) colocalizes with the α subunit[30] while immunolabelling of axons from knock-in mice show that β_1(CW) is retained in the AIS cytosol[7]. Although there seems to be a difference in membrane expression of β_1(CW) *in vitro* and *in vivo*, it is evident that the mutant protein is manufactured in both cases. The question remains then, is the increased thermosensitivity of this mutation due to a complete lack of association with the α subunit, thus removing the thermoprotective effect of β_1(WT)? Or does the mutation result in a unique alteration of channel function that is exacerbated at elevated temperatures?

My experiments show subtle differences between $Na_V1.2$ alone and $Na_V1.2$ + β_1(CW), comparable to previous observations in heterologous expression systems[27, 30-32], suggesting that β_1(CW) does associate with the α subunit. These results, then, point to a temperature-dependent increase in channel excitability due to altered modulation of channel function compared to β_1(WT). If, however, the β_1(CW) mutation results in a trafficking deficiency, as shown in the knock-in CW mouse model, then findings from this study can also be applicable towards other loss of function β_1 subunit mutations, such as R85H/C and R125C.

Because GEFS+ is a heterozygous genetic disorder, mutations to the SCN1B gene only affect one allele. This would result in only a portion of Na_V channels with no

associated β_1 subunit, while some would retain association with the wild-type β_1 subunit. Channels without associated β_1 subunit are hyperexcitable at elevated temperature. This could result in the channels with no associated β_1 subunit dominating membrane excitability at higher temperatures, thereby predisposing neurons to spontaneous action potential firing during febrile states.

Antiepileptic drugs (AEDs) targeted to Na_V channels are often administered to prevent or diminish such sustained, high frequency electrical activity. The individual response to such treatment, however, is highly variable among GEFS+ patients[88]. The variability in treatment response is likely attributable to the heterogeneous nature of GEFS+, as recent evidence suggests that the efficacy of AEDs is dependent on the individual's genotype[118]. The β_1(CW) mutation, for example, decreases channel sensitivity to phenytoin[96], and channels without an associated β_1 subunit have a reduced sensitivity to carbamezepine[109]. This reduction in drug sensitivity is thought to be caused by alterations to channel gating, and not by modification of the drug binding sites[96]. Since drug binding is highly dependent on channel kinetics, and temperature alters channel kinetics, it is not surprising that temperature affects drug binding as well. Although no studies to date have investigated the temperature-dependence of AEDs in neuronal channels, studies of antiarrythmic drug binding show that, at elevated temperature, there is a reduced frequency-dependent block of lidocaine[117], and an increased recovery from block from *O*-demethyl encainide[119].

These observations point to the importance of genetic background as well as environment on the efficacy of AEDs. The insights gained towards a GEFS+ mechanism from this study can aide in designing drugs specific to a patient's genotype. Such

individualized therapy can reduce potential side effects by having maximum efficacy during febrile episodes.

8: FUTURE DIRECTIONS

To better understand the biophysical mechanism behind the age-dependence of seizures in GEFS+ and FS patients, further experiments could be performed on the various developmentally regulated splice variants of neuronal Na_V channels. The temperature sensitivity of neonate and adult splice variants can be measured to determine if differential splicing plays a role in increasing the temperature threshold of the adult brain. The effect of the β_1(CW) mutation can also be assessed in conjunction with the two splice variants, as other FS mutations have been shown to have a differential effect depending on the variant in which they are expressed [47]. It would also be of value to test the efficacy of common AEDs used in treatment of GEFS+, such as carbamazepine, phenytoin, lacosamide, and lamotrigine, on channels co-expressing β_1(CW) at varying temperatures. If a temperature effect were observed, this would allow potential modification of dosage to increase drug potency depending on body temperature.

9: SUPPLEMENTARY FIGURES AND TABLES

Table 2. Compensation vs. no compensation

	Electrical compensation		**No compensation**	
	Tau 1	Tau 2	Tau 1	Tau 2
Values from individual experiments	0.128	15.37	0.039	8.83
	0.211	8.62	0.253	5.03
	0.273	14.12	0.525	11.08
			0.191	15.12
Mean	0.20462	12.7007	0.252037	10.0151
***p* value**	0.721		0.417	

Comparison of electrically compensated vs. non-compensated series resistance on fast and slow time constants of slow inactivation recovery at -90mV in $Na_V1.2 + \beta_1$(CW) at 34°C.

Table 3. Mean amplitude values

Mean ± SEM							
		22˚C			**34˚C**		
		$Na_V1.2$	$Na_V1.2+\beta_1$(WT)	$Na_V1.2+\beta_1$(CW)	$Na_V1.2$	$Na_V1.2+\beta_1$(WT)	$Na_V1.2+\beta_1$(CW)
+10mV SI onset	A_1	0.60 ± 0.091	0.27 ± 0.077	0.52± 0.091	0.58 ± 0.091	0.54 ± 0.091	0.53 ± 0.091
	A_2^*	0.38 ± 0.081	0.69 ± 0.068	0.51 ± 0.081	0.28 ± 0.081	0.33 ± 0.081	0.39 ± 0.081
-90mV SI recovery	A_1	-0.35 ± 0.039	-0.38 ± 0.038	-0.31 ± 0.035	-0.35 ± 0.038	-0.33 ± 0.038	-0.29 ± 0.033
	A_2	-0.61 ± 0.064	-0.62 ± 0.064	-0.64 ± 0.059	-0.51 ± 0.064	-0.62 ± 0.064	-0.56 ± 0.054
UDI	A_1^*	0.23 ± 0.044	0.36 ± 0.038	0.30 ± 0.044	0.16 ± 0.048	0.21 ± 0.048	0.15 ± 0.040
	A_2^*	0.48 ± 0.046	0.29 ± 0.040	0.40 ± 0.046	0.30 ± 0.051	0.27 ± 0.051	0.21 ± 0.043
-60mV FI recovery	A_1	-0.71 ± 0.065	-0.67 ± 0.055	-0.57 ± 0.060	-0.75 ± 0.065	-0.70 ± 0.065	-0.77 ± 0.065
	A_2	-0.29 ± 0.067	-0.35 ± 0.056	-0.43 ± 0.061	-0.24 ± 0.067	-0.34 ± 0.067	-0.25 ± 0.067

Mean amplitude values A_1 and A_2 of respective time constants τ_1 and τ_2 as derived from double exponential fits to normalized current amplitude. Asterisks indicate significant difference at 22°C and 34°C among averaged values for all subunits at $p<0.01$.

Supplementary Figure 1. Log plot of FI recovery

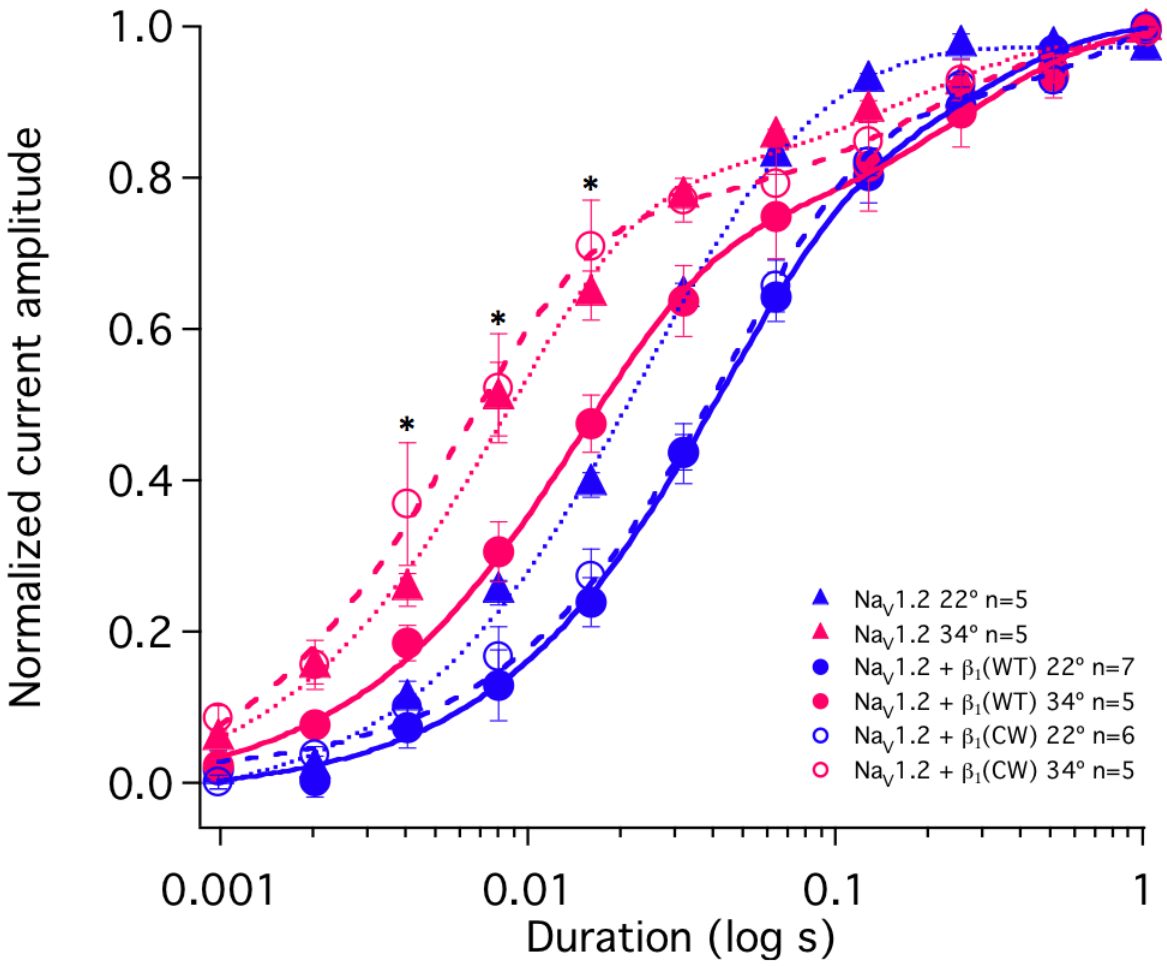

Log plot of fast inactivation recovery at -60mV. Voltage protocol as described in methods. Normalized current amplitude is plotted against the log of the duration of recovery pulse to illustrate bi-exponential component of fit. Asterisks indicate significant difference in normalized current amplitude at 34°C between $Na_V1.2 + \beta_1$(WT) and $Na_V1.2 + \beta_1$(CW) ($p<0.01$).

10: REFERENCES

1. Stafstrom CE. The incidence and prevalence of febrile seizures. In: *Febrile Seizures*. Editors: Baram TZ, Shinnar S. San Diego, CA: Academic Press; 2002. p. 1–21.

2. Waruiru C, Appleton R. Febrile seizures: an update. *Arch Dis Child* 2004;89(8):751.

3. Jensen FE, Sanchez RM. Why does the developing brain demonstrate heightened susceptibility to febrile and other provoked seizures?. *Febrile Seizures*:153–168.

4. Berkovic SF, Petrou S. Febrile seizures: traffic slows in the heat. *Trends Mol Med* 2006; 8;12(8):343-344.

5. Guidelines for epidemiologic studies on epilepsy: commission on epidemiology and - prognosis, International League Against Epilepsy. *Epilepsia* 1993;34(4):592-596.

6. Hille B. *Ion channels of excitable membranes.* 3rd ed. Sunderland, MA: Sinauer Associates; 2001.

7. Wimmer VC, Reid CA, Mitchell S, Richards KL, Scaf BB, Leaw BT, et al. Axon initial segment dysfunction in a mouse model of genetic epilepsy with febrile seizures plus. *J Clin Invest* 2010;120(8): 2661–2671

8. Thomas EA, Hawkins RJ, Richards KL, Xu R, Gazina EV, Petrou S. Heat opens axon initial segment sodium channels: A febrile seizure mechanism?. *Ann Neurol* 2009;66(2):219-226.

9. Ruff RL. Effects of temperature on slow and fast inactivation of rat skeletal muscle Na+ channels. *Am J Physiol Cell Physiol* 1999; November 1;277(5):937-947.

10. Schwarz JR. The effect of temperature on Na currents in rat myelinated nerve fibres. *Pflügers Archiv Eur J of Physy* 1986;406(4):397-404.

11. Dice MS, Abbruzzese JL, Wheeler JT, Groome JR, Fujimoto E, Ruben PC. Temperature-sensitive defects in paramyotonia congenita mutants R1448C and T1313M. *Muscle Nerve* 2004;30(3):277-288

12. Carle T, Fournier E, Sternberg D, Fontaine B, Tabti N. Cold-induced disruption of Na channel slow inactivation underlies paralysis in highly thermosensitive paramyotonia. *J Physiol (Lond)* 2009;587(8):1705-1714.

13. Webb J, Cannon SC. Cold-induced defects of sodium channel gating in atypical periodic paralysis plus myotonia. *Neurology* 2008;70(10):755-761.

14. Stafstrom CE. Persistent sodium current and its role in epilepsy. *Epilepsy Currents* 2007;7(1):15-22.

15. Bénitah JP, Chen Z, Balser JR, Tomaselli GF, Marbán E. Molecular dynamics of the sodium channel pore vary with gating: interactions between P-segment motions and inactivation. *The Journal of Neuroscience* 1999;19(5):1577-1585

16. Kambouris NG, Hastings LA, Stepanovic S, Marban E, Tomaselli GF, Balser JR. Mechanistic link between lidocaine block and inactivation probed by outer pore mutations in the rat μ1 skeletal muscle sodium channel. *J Physiol (Lond)* 1998;512(3):693-705.

17. Vilin YY, Ruben PC. Slow inactivation in voltage-gated sodium channels. *Cell Biochem Biophys* 2001;35(2):171-190.

18. Jones DK, Ruben PC. Biophysical defects in voltage-gated sodium channels associated with long QT and Brugada syndromes. *Channels (Austin)* 2008; Mar 18;2(2):70-80

19. Ulbricht W. Sodium channel inactivation: molecular determinants and modulation. *Physiol Rev* 2005;85(4):1271-1301

20. Brackenbury WJ, Isom LL. Voltage-gated Na channels: Potential for β subunits as therapeutic targets. *Expert Opinion on Therapeutic Targets* 2008;12(9):1191-1203.

21. Qu Y, Curtis R, Lawson D, Gilbride K, Ge P, DiStefano PS, et al. Differential modulation of sodium channel gating and persistent sodium currents by the β1, β2, and β3 Subunits. *Molecular and Cellular Neuroscience* 2001; 11;18(5):570-580.

22. Qu Y, Rogers JC, Chen SF, McCormick KA, Scheuer T, Catterall WA. Functional roles of the extracellular segments of the sodium channel α subunit in voltage-dependent gating and modulation by β1 subunits. *J Biol Chem* 1999;274(46):32647-32654

23. Makita N, Bennett PB, George Jr AL. Molecular determinants of beta 1 subunit-induced gating modulation in voltage-dependent Na channels. *Journal of Neuroscience* 1996;16(22):7117-7127.

24. Meadows L, Malhotra JD, Stetzer A, Isom LL, Ragsdale DS. The intracellular segment of the sodium channel β1 subunit is required for its efficient association with the channel α subunit. *J Neurochem* 2001;76(6):1871-1878.

25. An R, Wang X, Kerem B, Benhorin J, Medina A, Goldmit M, et al. Novel LQT-3 mutation affects Na channel activity through interactions between {alpha}-and ß1 use-dependent inactivation s. *Circ Res* 1998;83(2):141-146.

26. Spampanato J, Kearney J, De Haan G, McEwen D, Escayg A, Aradi I, et al. A novel epilepsy mutation in the sodium channel SCN1A identifies a cytoplasmic domain for {beta} subunit interaction. *Journal of Neuroscience* 2004;24(44):10022-10034.

27. Moran O, Conti F. Skeletal Muscle Sodium Channel Is Affected by an Epileptogenic [beta] 1 Subunit Mutation. *Biochem Biophys Res Commun* 2001;282(1):55-59.

28. Qu Y, Curtis R, Lawson D, Gilbride K, Ge P, DiStefano PS, et al. Differential modulation of sodium channel gating and persistent sodium currents by the β1, β2, and β3 subunits. *Molecular and Cellular Neuroscience* 2001; 11;18(5):570-580.

29. Wright SN, Wang SY, Xiao YF, Wang GK. State-dependent cocaine block of sodium channel isoforms, chimeras, and channels coexpressed with the [beta] 1 subunit. *Biophys J* 1999;76(1):233-245.

30. Meadows LS, Malhotra J, Loukas A, Thyagarajan V, Kazen-Gillespie KA, Koopman MC, et al. Functional and biochemical analysis of a sodium channel beta 1 subunit Mutation responsible for generalized epilepsy with febrile seizures plus type 1. *J Neurosci* 2002; December 15;22(24):10699-10709.

31. Tammaro P, Conti F, Moran O. Modulation of sodium current in mammalian cells by an epilepsy-correlated β1-subunit mutation. *Biochem Biophys Res Commun* 2002; 3/8;291(4):1095-1101.

32. Aman TK, Grieco-Calub TM, Chen C, Rusconi R, Slat EA, Isom LL, et al. Regulation of persistent Na current by interactions between {beta} subunits of voltage-gated Na channels. *J Neurosci* 2009; February 18;29(7):2027-2042.

33. Xu R, Thomas EA, Gazina EV, Richards KL, Quick M, Wallace RH, et al. Generalized epilepsy with febrile seizures plus–associated sodium channel β1 subunit mutations severely reduce beta subunit–mediated modulation of sodium channel function. *Neuroscience* 2007; 8/10;148(1):164-174.

34. Isom LL, Scheuer T, Brownstein AB, Ragsdale DS, Murphy BJ, Catterall WA. Functional co-expression of the beta1 and type IIA alpha subunits of sodium channels in a mammalian cell line. *J Biol Chem* 1995;270(7):3306-3312.

35. Isom L, De Jongh K, Patton D, Reber B, Offord J, Charbonneau H, et al. Primary structure and functional expression of the beta 1 subunit of the rat brain sodium channel. *Science* 1992;256(5058):839-842.

36. Meadows LS, Chen YH, Powell AJ, Clare JJ, Ragsdale DS. Functional modulation of human brain Nav1.3 sodium channels, expressed in mammalian cells, by auxiliary β1, β2 and β3 subunits. *Neuroscience* 2002; 10/11;114(3):745-53.

37. Webb J, Wu F, Cannon SC. Slow inactivation of the NaV1. 4 sodium channel in mammalian cells is impeded by co-expression of the β1 subunit. *Pflügers Archiv European Journal of Physiology* 2009;457(6):1253-1263.

38. Valdivia CR, Nagatomo T, Makielski JC. Late Na currents affected by [alpha] subunit isoform and [beta] 1 subunit co-expression in HEK293 cells. *J Mol Cell Cardiol* 2002;34(8):1029-1039.

39. Chen C, Westenbroek RE, Xu X, Edwards CA, Sorenson DR, Chen Y, et al. Mice lacking sodium channel {beta}1 subunits display defects in neuronal excitability, sodium channel expression, and nodal architecture. *J Neurosci* 2004; April 21;24(16):4030-4042.

40. Watanabe H, Koopmann TT, Le Scouarnec S, Yang T, Ingram CR, Schott JJ, et al. Sodium channel β1 subunit mutations associated with Brugada syndrome and cardiac conduction disease in humans. *J Clin Invest* 2008;118(6):2260-2268.

41. Wallace RH, Wang DW, Singh R, Scheffer IE, George Jr AL, Phillips HA, et al. Febrile seizures and generalized epilepsy associated with a mutation in the Na-channel beta1 subunit gene SCN1B. *Nat Genet* 1998;19(4):366-370.

42. Scheffer IE, Harkin LA, Grinton BE, Dibbens LM, Turner SJ, Zielinski MA, et al. Temporal lobe epilepsy and GEFS+ phenotypes associated with SCN1B mutations. *Brain* 2007; January 1;130(1):100-109.

43. Colbert CM, Pan E. Ion channel properties underlying axonal action potential initiation in pyramidal neurons. *Nat Neurosci* 2002;5(6):533-538.

44. Palmer LM, Stuart GJ. Site of action potential initiation in layer 5 pyramidal neurons. *Journal of Neuroscience* 2006;26(6):1854-1863.

45. Kole MHP, Ilschner SU, Kampa BM, Williams SR, Ruben PC, Stuart GJ. Action potential generation requires a high sodium channel density in the axon initial segment. *Nat Neurosci* 2008;11(2):178-186.

46. Hu W, Tian C, Li T, Yang M, Hou H, Shu Y. Distinct contributions of Nav1. 6 and Nav1. 2 in action potential initiation and backpropagation. *Nat Neurosci* 2009;12(8):996-1002.

47. Xu R, Thomas EA, Jenkins M, Gazina EV, Chiu C, Heron SE, et al. A childhood epilepsy mutation reveals a role for developmentally regulated splicing of a sodium channel. *Molecular and Cellular Neuroscience* 2007; 6;35(2):292-301.

48. Aronica E, Yankaya B, Troost D, van Vliet EA, da Silva FHL, Gorter JA. Induction of neonatal sodium channel II and III α-isoform mRNAs in neurons and microglia after status epilepticus in the rat hippocampus. *Eur J Neurosci* 2001;13(6):1261-1266.

49. Whitaker WRJ, Faull RLM, Dragunow M, Mee EW, Emson PC, Clare JJ. Changes in the mRNAs encoding voltage-gated sodium channel types II and III in human epileptic hippocampus. *Neuroscience* 2001; 9/6;106(2):275-285.

50. Guo F, Yu N, Cai J, Quinn T, Zong Z, Zeng Y, et al. Voltage-gated sodium channel Nav1.1, Nav1.3 and β1 subunit were up-regulated in the hippocampus of spontaneously epileptic rat. *Brain Res Bull* 2008; 1/31;75(1):179-187.

51. Willow M, Taylor SM, Catterall WA, Finnell RH. Down regulation of sodium channels in nerve terminals of spontaneously epileptic mice. *Cell Mol Neurobiol* 1986;6(2):213-220.

52. Pröbstel T, Rüdel R, Ruppersberg J. Hodgkin-Huxley parameters of the sodium channels in human myoballs. *Eur J Phys* 1988;412(3):264-269.

53. Hodgkin A, Katz B. The effect of temperature on the electrical activity of the giant axon of the squid. *J Physiol (Lond)* 1949;109(1-2):240-249.

54. Kohlhardt M. Different temperature sensitivity of cardiac Na channels in cell-attached and cell-free conditions. *Am J Phys - Cell Phys*1990;259(4):C599-C604.

55. Keller DI, Rougier JS, Kucera JP, Benammar N, Fressart V, Guicheney P, et al. Brugada syndrome and fever: genetic and molecular characterization of patients carrying SCN5A mutations. *Cardiovasc Res* 2005;67(3):510-519.

56. Colatsky T. Voltage clamp measurements of sodium channel properties in rabbit cardiac Purkinje fibres. *J Physiol (Lond)* 1980;305(1):215-234.

57. Keller DI, Huang H, Zhao J, Frank R, Suarez V, Delacrétaz E, et al. A novel SCN5A mutation, F1344S, identified in a patient with Brugada syndrome and fever-induced ventricular fibrillation. *Cardiovasc Res* 2006;70(3):521-529.

58. Samani K, Wu G, Ai T, Shuraih M, Mathuria NS, Li Z, et al. A novel SCN5A mutation V1340I in Brugada syndrome augmenting arrhythmias during febrile illness. *Heart Rhythm* 2009;6(9):1318-1326.

59. Mohammadi B, Mitrovic N, Lehmann-Horn F, Dengler R, Bufler J. Mechanisms of cold sensitivity of paramyotonia congenita mutation R1448H and overlap syndrome mutation M1360V. *J Physiol (Lond)* 2003;547(3):691-698.

60. Nagatomo T, Fan Z, Ye B, Tonkovich GS, January CT, Kyle JW, et al. Temperature dependence of early and late currents in human cardiac wild-type and long QT Delta KPQ Na channels. *Am J Phys - Heart and Circ Phys*1998;275(6):H2016-H2024.

61. Murray KT, Anno T, Bennett PB, Hondeghem LM. Voltage clamp of the cardiac sodium current at 37 degrees C in physiologic solutions. *Biophys J* 1990;57(3):607-613.

62. Irvine LA, Saleet Jafri M, Winslow RL. Cardiac sodium channel Markov model with temperature dependence and recovery from inactivation. *Biophys J* 1999;76(4):1868-1885.

63. Webb J, Cannon SC. Cold-induced defects of sodium channel gating in atypical periodic paralysis plus myotonia. *Neurology* 2008;70(10):755-761.

64. Berg AT, Shinnar S, Levy SR, Testa FM. Childhood-onset epilepsy with and without preceding febrile seizures. *Neurology* 1999;53(8):1742.

65. Johnson E, Dubovsky J, Rich S, O'Donovan C, Orr H, Anderson V, et al. Evidence for a novel gene for familial febrile convulsions, FEB2, linked to chromosome 19p in an extended family from the Midwest. *Hum Mol Genet* 1998;7(1):63.

66. Nabbout R, Prud'homme JF, Herman A, Feingold J, Brice A, Dulac O, et al. A locus for simple pure febrile seizures maps to chromosome 6q22-q24. *Brain* 2002;125(12):2668-2680.

67. Nakayama J, Yamamoto N, Hamano K, Iwasaki N, Ohta M, Nakahara S, et al. Linkage and association of febrile seizures to the IMPA2 gene on human chromosome 18. *Neurology* 2004;63(10):1803-1807.

68. Hedera P, Ma S, Blair MA, Taylor KA, Hamati A, Bradford Y, et al. Identification of a novel locus for febrile seizures and epilepsy on chromosome 21q22. *Epilepsia* 2006;47(10):1622-1628.

69. Nabbout R, Baulac S, Desguerre I, Bahi-Buisson N, Chiron C, Ruberg M, et al. New locus for febrile seizures with absence epilepsy on 3p and a possible modifier gene on 18p. *Neurology* 2007;68(17):1374-1381.

70. Dai XH, Chen WW, Wang X, Zhu QH, Li C, Li L, et al. A novel genetic locus for familial febrile seizures and epilepsy on chromosome 3q26. 2–q26. 33. *Hum Genet* 2008;124(4):423-429.

71. Mantegazza M, Gambardella A, Rusconi R, Schiavon E, Annesi F, Cassulini RR, et al. Identification of an Nav1. 1 sodium channel (SCN1A) loss-of-function mutation associated with familial simple febrile seizures. *Proceedings of the National Academy of Sciences* 2005;102(50):18177-18182.

72. Schlachter K, Gruber-Sedlmayr U, Stogmann E, Lausecker M, Hotzy C, Balzar J, et al. A splice site variant in the sodium channel gene SCN1A confers risk of febrile seizures. *Neurology* 2009;72(11):974-978.

73. Deprez L, Claes LRF, Claeys KG, Audenaert D, Van Dyck T, Goossens D, et al. Genome-wide linkage of febrile seizures and epilepsy to the FEB4 locus at 5q14. 3-q23. 1 and no MASS1 mutation. *Hum Genet* 2006;118(5):618-625.

74. Dube C, Vezzani A, Behrens M, Bartfai T, Baram TZ, Foundation E. Interleukin-1b contributes to the generation of experimental febrile seizures. *Ann Neurol* 2005;57(1):152-155.

75. Kiviranta T, Tuomisto L, Airaksinen EM. Osmolality and electrolytes in cerebrospinal fluid and serum of febrile children with and without seizures. *Eur J Pediatr* 1996;155(2):120-125.

76. Schuchmann S, Vanhatalo S, Kaila K. Neurobiological and physiological mechanisms of fever-related epileptiform syndromes. *Brain and Development* 2009;31(5):378-382.

77. Schuchmann S, Tolner EA, Marshall P, Vanhatalo S, Kaila K. Pronounced increase in breathing rate in the" hair dryer model" of experimental febrile seizures. *Epilepsia* 2008;49(5):926-928.

78. Tapia R. Putting the heat on febrile seizures. *Nat Med* 2006;12(7):729-730.

79. Berg AT. Are febrile seizures provoked by a rapid rise in temperature?. *Archives of Pediatrics and Adolescent Medicine* 1993;147(10):1101-1103.

80. Morimoto T, Nagao H, Sano N, Takahashi M, Matsuda H. Electroencephalographic study of rat hyperthermic seizures. *Epilepsia* 1991;32(3):289-293.

81. McCaughran Jr JA, Schechter N. Experimental febrile convulsions: long-term effects of hyperthermia-induced convulsions in the developing rat. *Epilepsia* 1982;23(2):173-183.

82. Baram TZ, Gerth A, Schultz L. Febrile seizures: an appropriate-aged model suitable for long-term studies. *Dev Brain Res* 1997;98(2):265-270.

83. Holtzman D, Obana K, Olson J. Hyperthermia-induced seizures in the rat pup: a model for febrile convulsions in children. *Science* 1981;213:1034-1036.

84. Dube C, Chen K, Eghbal-Ahmadi M, Brunson K, Soltesz I, Baram TZ. Prolonged febrile seizures in the immature rat model enhance hippocampal excitability long term. *Ann Neurol* 2000;47(3):336-344.

85. Tancredi V, D'Arcangelo G, Zona C, Siniscalchi A, Avoli M. Induction of epileptiform activity by temperature elevation in hippocampal slices from young rats: an in vitro model for febrile seizures?. *Epilepsia* 2005;33(2):228-234.

86. Scheffer IE, Harkin LA, Dibbens LM, Mulley JC, Berkovic SF. Neonatal epilepsy syndromes and generalized epilepsy with febrile seizures plus (GEFS). *Epilepsia* 2005;46(s10):41-47.

87. Scheffer IE, Zhang YH, Jansen FE, Dibbens L. Dravet syndrome or genetic (generalized) epilepsy with febrile seizures plus?. *Brain and Development* 2009;31(5):394-400.

88. Scheffer I, Berkovic S. Generalized epilepsy with febrile seizures plus. A genetic disorder with heterogeneous clinical phenotypes. *Brain* 1997;120(3):479-490.

89. Baulac S, Huberfeld G, Gourfinkel-An I, Mitropoulou G, Beranger A, Prud'homme JF, et al. First genetic evidence of GABAA receptor dysfunction in epilepsy: a mutation in the γ2-subunit gene. *Nat Genet* 2001;28(1):46-48.

90. Dibbens LM, Feng HJ, Richards MC, Harkin LA, Hodgson BL, Scott D, et al. GABRD encoding a protein for extra-or peri-synaptic GABAA receptors is a susceptibility locus for generalized epilepsies. *Hum Mol Genet* 2004;13(13):1315-1319.

91. Singh NA, Pappas C, Dahle EJ, Claes LRF, Pruess TH, De Jonghe P, et al. A Role of SCN9A in Human Epilepsies, As a Cause of Febrile Seizures and As a Potential Modifier of Dravet Syndrome. *Plos Genetics* 2009;5(9):e1000649

92. Meisler M, Kearney J. Sodium channel mutations in epilepsy and other neurological disorders. *J Clin Invest* 2005; 115(8):2010-2017.

93. Rush AM, Dib-Hajj SD, Liu S, Cummins TR, Black JA, Waxman SG. A single sodium channel mutation produces hyper-or hypoexcitability in different types of neurons. *National Acad Sciences* 2006;103(21):8245-8250

94. Patino GA, Claes LRF, Lopez-Santiago LF, Slat EA, Dondeti RSR, Chen C, et al. A functional null mutation of SCN1B in a patient with Dravet syndrome. *Journal of Neuroscience* 2009;29(34):10764-10778.

95. Meadows LS, Chen YH, Powell AJ, Clare JJ, Ragsdale DS. Functional modulation of human brain Nav1.3 sodium channels, expressed in mammalian cells, by auxiliary β1, β2 and β3 subunits. *Neuroscience* 2002; 10/11;114(3):745-753.

96. Lucas PT, Meadows LS, Nicholls J, Ragsdale DS. An epilepsy mutation in the [beta] 1 subunit of the voltage-gated sodium channel results in reduced channel sensitivity to phenytoin. *Epilepsy Res* 2005;64(3):77-784.

97. Isom LL. Sodium Channel {beta} Subunits: Anything but Auxiliary. *Neuroscientist* 2001; February 1;7(1):42-54.

98. Garrido JJ, Giraud P, Carlier E, Fernandes F, Moussif A, Fache MP, et al. A targeting motif involved in sodium channel clustering at the axonal initial segment. *Science* 2003;300(5628):2091-2094.

99. Kiernan MC, Krishnan AV, Lin CSY, Burke D, Berkovic SF. Mutation in the Na channel subunit SCN1B produces paradoxical changes in peripheral nerve excitability. *Brain* 2005;128(8):1841-1846.

100. Patino GA, Isom LL. Electrophysiology and beyond: Multiple roles of Na channel [beta] subunits in development and disease. *Neurosci Lett* 2010;486(2):53-59.

101. Isom LL, Scheuer T, Brownstein AB, Ragsdale DS, Murphy BJ, Catterall WA. Functional co-expression of the 1 and type IIA subunits of sodium channels in a mammalian cell line. *J Biol Chem* 1995;270(7):3306-3312.

102. Moran O, Nizzari M, Conti F. Endogenous expression of the [beta] 1A sodium channel subunit in HEK-293 cells. *FEBS Lett* 2000;473(2):132-134.

103. Xie X, Lancaster B, Peakman T, Garthwaite J. Interaction of the antiepileptic drug lamotrigine with recombinant rat brain type IIA Na channels and with native Na channels in rat hippocampal neurones. *Archiv Eur J Phy* 1995;430(3):437-446.

104. Fleischhauer R, Mitrovic N, Deymeer F, Lehmann-Horn F, Lerche H. Effects of temperature and mexiletine on the F1473S Na channel mutation causing paramyotonia congenita. *Archiv Eur J Phy* 1998;436(5):757-765.

105. Coste B, Osorio N, Padilla F, Crest M, Delmas P. Gating and modulation of presumptive NaV1. 9 channels in enteric and spinal sensory neurons. *Molecular and Cellular Neuroscience* 2004;26(1):123-134.

106. Buffer reference center. Available at: http://www.sigmaaldrich.com/life-science/core-bioreagents/biological-buffers/learning-center/buffer-reference-center.html. Accessed March/28, 2011.

107. Vilin Y, Ruben P. Differential pH-dependent regulation of NaV channels. *Biophys* J *abstract*, 2010; Pos 581.

108. Xie X, Dale TJ, John VH, Cater HL, Peakman TC, Clare JJ. Electrophysiological and pharmacological properties of the human brain type IIA Na channel expressed in a stable mammalian cell line. *Archiv Eur J Phy* 2001;441(4):425-433.

109. Uebachs M, Opitz T, Royeck M, Dickhof G, Horstmann MT, Isom LL, et al. Efficacy loss of the anticonvulsant carbamazepine in mice lacking sodium channel β subunits via paradoxical effects on persistent sodium currents. *The Journal of Neuroscience* 2010;30(25):8489-8501.

110. Ellerkmann RK, Riazanski V, Elger CE, Urban BW, Beck H. Slow recovery from inactivation regulates the availability of voltage-dependent Na channels in hippocampal granule cells, hilar neurons and basket cells. *J Physiol (Lond)* 2001;532(2):385-397.

111. Webb J. Slow inactivation of the NaV1. 4 sodium channel in mammalian cells is impeded by co-expression of the beta1 subunit. *Archiv Eur J Phy* 2009; 04/00;457(6):1253-1263.

112. Sugiura Y, Makita N, Li L, Noble P, Kimura J, Kumagai Y, et al. Cold induces shifts of voltage dependence in mutant SCN4A, causing hypokalemic periodic paralysis. *Neurology* 2003;61(7):914-918.

113. Vilin YY, Makita N, George Jr AL, Ruben PC. Structural determinants of slow inactivation in human cardiac and skeletal muscle sodium channels. *Biophys J* 1999;77(3):1384-1393.

114. Townsend C, Horn R. Effect of alkali metal cations on slow inactivation of cardiac Na channels. *J Gen Physiol* 1997;110(1):23-33.

115. Villalba-Galea CA, Sandtner W, Starace DM, Bezanilla F. S4-based voltage sensors have three major conformations. *Proceedings of the National Academy of Sciences* 2008;105(46):17600-17607.

116. Wang DW, Makita N, Kitabatake A, Balser JR, George Jr AL. Enhanced Na channel intermediate inactivation in Brugada syndrome. *Circ Res* 2000;87(8):e37-e43.

117. Makielski J, Falleroni M. Temperature dependence of sodium current block by lidocaine in cardiac Purkinje cells. *Am J Phy - Heart and Circulatory Physiology* 1991;260(3):H681-H689.

118. Grover S, Gourie-Devi M, Baghel R, Sharma S, Bala K, Gupta M, et al. Genetic profile of patients with epilepsy on first-line antiepileptic drugs and potential directions for personalized treatment. *Pharmacogenomics* 2010;11(7):927-941.

119. Johns JA, Anno T, Bennett PB, Snyders DJ, Hondeghem LM. Temperature and voltage dependence of sodium channel blocking and unblocking by O-demethyl encainide in isolated guinea pig myocytes. *J Cardiovasc Pharmacol* 1989;13(6):826-835.

120. Silva, JR., Goldstein, SAN. Slow inactivation of NaV channels described by composite movements of voltage sensors in domains I, II and III. *Biophys J abstract* 2011;100(3):15a-15a

121. DeCaen PG, Yarov-Yarovoy V, Sharp EM, Scheuer T, Catterall WA. Sequential formation of ion pairs during activation of a sodium channel voltage sensor. *Proceedings of the National Academy of Sciences* 2009;106(52):22498-22503.

122. Audenaert D, Claes L, Ceulemans B, Löfgren A, Van Broeckhoven C, De Jonghe P. A deletion in SCN1B is associated with febrile seizures and early-onset absence epilepsy. *Neurology* 2003;61(6):854-856.